GEOLOGICAL SURVEY OF CANADA
OPEN FILE 7370

Geological setting of banded iron formation-hosted gold mineralization in the Geraldton area, Northern Ontario: preliminary results

Z. Tòth, B. Lafrance, B. Dubé, P. Mercier-Langevin, and V. McNicoll

2013

Natural Resources Canada Ressources naturelles Canada

Canada

GEOLOGICAL SURVEY OF CANADA
OPEN FILE 7370

Geological setting of banded iron formation-hosted gold mineralization in the Geraldton area, Northern Ontario: preliminary results

Z. Tòth[1], B. Lafrance[1], B. Dubé[2], P. Mercier-Langevin[2], and V. McNicoll[3]

[1] Laurentian University, 933 Ramsey Road, Sudbury ON P3E 2C6
[2] Geological Survey of Canada, 490 rue de la Couronne, Québec QC G1K 9A9
[3] Geological Survey of Canada, 601 Booth Street, Ottawa ON K1A 0E8

2013

doi:10.4095/292558

This publication is available for free download through GEOSCAN (http://geoscan.ess.nrcan.gc.ca/).

Recommended citation
Tòth, Z., Lafrance, B., Dubé, B., Mercier-Langevin, P., and McNicoll, V., 2013. Geological setting of banded iron formation-hosted gold mineralization in the Geraldton area, Northern Ontario: preliminary results; Geological Survey of Canada, Open File 7370, 54 p. doi:10.4095/292558

Publications in this series have not been edited; they are released as submitted by the author

Open File Report

Targeted Geoscience Initiative 4. Lode Gold Deposits in Ancient Deformed and Metamorphosed Terranes

Geological Setting of Banded Iron Formation–Hosted Gold Mineralization in the Geraldton Area, Northern Ontario: Preliminary Results

Z. Tòth, B. Lafrance, B. Dubé, P. Mercier-Langevin, and V. McNicoll

General Introduction

The characterization of banded iron formation (BIF)-hosted gold ore systems is one of the main theme of the Targeted Geoscience Initiative-4 Lode Gold project of the Geological Survey of Canada (Dubé et al. 2011). The Geraldton area was selected as one of four areas to study these systems because of the excellent exposure, easy accessibility, and availability of new exploration data and drill cores. This project started on July 15th, 2012 and is carried out as a collaboration between the Geological Survey of Canada, the Ontario Geological Survey, and Premier Gold Mines Limited.

The report is divided in four sections. The first section summarizes the results of the summer's field work and describes the relationships between structural features, rock types, and mineralization. The second section presents observations from four drill holes that intersected the F Zone and North Zone, which are the main mineralized zones in the Geraldton area. The detailed drill logs are included in Appendix. The third section describes the petrography of four thin sections from the F Zone and North Zone. The fourth section reports preliminary results on the geochemistry of the alteration envelopes surrounding the mineralized zones. The last section summarizes the results of the study.

Structural and Lithological Controls on Banded Iron Formation–Hosted Gold Mineralization in the Geraldton Area, northern Ontario

Introduction

Banded iron formation-hosted deposits in the Geraldton area have been described by Pye (1952), Horwood and Pye (1955) and Macdonald (1988). Since then, extensive exploration activities have produced numerous new exposures as well as multiple new drill hole sections across the deposits. The project began during the summer 2012 with detailed mapping of two new large stripped outcrops, the Portal stripping and the Tombill Bankfield Fault stripping. The preliminary results of the mapping are presented in this report and in the Summary of Field Work and Other Activities 2012 volume of the Ontario Geological Survey (Lafrance et al. 2012).

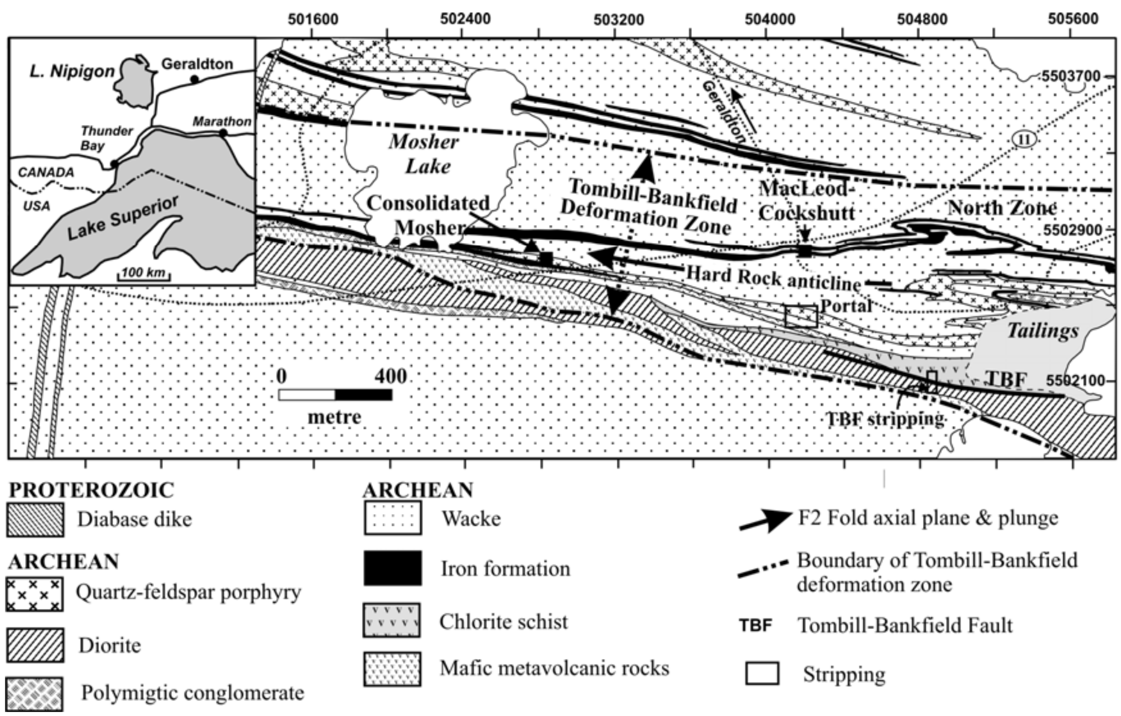

Figure 1: Simplified geological map of the Geraldton area after Horwood and Pye (1955) and Pye (1952) with modifications by authors. UTM coordinates are based on North American Datum 1927, Zone 16. Inset map shows the location of Geraldton.

Background

The Geraldton area is located east of Lake Nipigon in the eastern part of the Beardmore-Geraldton Belt (BGB) along the southern margin of the Wabigoon Subprovince of the Archean Superior Province (Figure 1). The BGB comprises three metasedimentary rock panels (southern, central, and northern sedimentary units) that are fault-bounded and interleaved with three volcanic rock panels (southern, central, and northern volcanic units). The southern volcanic unit has MORB geochemical affinity and it represents ocean floor crust that formed south of an oceanic island arc (central volcanic unit) and back-arc basin (northern volcanic unit) (Tomlinson et al. 1986). A felsic flow and a synvolcanic dike in the central and northern volcanic units, respectively, have U-Pb zircon crystallization ages of 2724.9±1.2 Ma (Hart et al. 2002). Thus, these two volcanic units stood 2725 Ma ago as an island arc and back-arc system outboard and south of the Wabigoon. The three volcanic units collided and were accreted to the southern margin of the Wabigoon prior to the deposition of the sedimentary units at ca. 2696 Ma to ca. 2691 Ma (Lafrance et al. 2004). From north to south, the sedimentary units record progressively deeper depositional environments. They were emplaced unconformably above the volcanic units as fluvial to alluvial fan deposits (northern sedimentary unit), deltaic to subaqueous fan deposits (central sedimentary unit), and deeper water turbidite deposits (southern sedimentary unit) (Devaney and Williams 1989). They represent a southward prograding clastic wedge that was fed by the erosion of the uplifted Wabigoon (Devaney and Williams 1989).

Thrust imbrications of the volcanic and sedimentary units began shortly after deposition of the sedimentary units during an early D_1 deformation event (Devaney and Williams 1989; Lafrance et al. 2004). Rare isoclinal F_1 folds are the only manifestation of D_1 as structural contacts and possible thrust faults between volcanic and sedimentary units were later reactivated as transcurrent shear zones. During D_2 north-south compression, the southern sedimentary unit was regionally folded into tight to isoclinal, E-striking, F_2 folds with an axial planar S_2 cleavage (Lafrance et al. 2004). S_2 is oriented at high angle to bedding in F_2 fold hinges and is generally parallel to bedding along the limbs of the folds. S_2 is expressed by the flattening of clasts and pillows in the volcanic units and by a bedding-parallel cleavage in the central and northern sedimentary units. Late, regional, D_3 dextral transpression, produced most penetrative structures in the belt. During D_3, F_2 and S_2 were folded by outcrop- to map-scale, west-plunging, Z-shaped F_3 folds. The D_2 structures were overprinted by a regional S_3 cleavage oriented anticlockwise to bedding, and they were transected by east-trending, dextral, transcurrent D_3 shear zones (Lafrance et al. 2004). F_3 and S_3 are in turn overprinted by Z-shaped F_3' folds and associated S_3' cleavage, which formed during the same progressive D_3 deformation event (Lafrance et al. 2004). Felsic porphyry dikes and sills with a U-Pb crystallization age of 2691 +3/-2 Ma (Anglin 1987; Anglin et al. 1987) are folded by F_2 and overprinted by S_3, providing a maximum deformation age of ca. 2691 Ma for both D_2 and D_3.

All past-producing gold mines in the Geraldton area (e.g. Little Long Lac, Hardrock, MacLeod-Cockshutt, Consolidated Mosher, Magnet, Bankfield) are in the southern sedimentary unit. Most ore zones are hosted in a 1 km-wide high-strain zone, called the Tombill-Bankfield deformation zone (Figure 1.), located close to the contact between the southern sedimentary unit and the Quetico sedimentary rocks to the South (Lafrance et al. 2004). A discrete fault zone defined by brecciated rocks known as the Tombill-Bankfield fault, occurs within the wider, more ductile, deformation zone. The deposits hosted by the deformation zone collectively produced 2.36 million ounces of gold (Mason and White 1986). Gold occurs in sulphide-rich replacement lenses and quartz-carbonate veins in the hinge of F_2 and F_3 folded iron formation (e.g. North Zone). It also occurs in quartz veins and associated sericitic selvages in folded porphyry bodies and in wacke near or at the contact with porphyry (e.g. F Zone) (Horwood and Pye 1955). It is further found in quartz stringer zones within wacke and diorite (Horwood and Pye 1955). Gold mineralization is interpreted to be syn-D_3 and to have been emplaced in faults, shear zones, and fractures that formed along sheared contacts and across the hinge of F_2 and F_3 folds (Anglin 1987; Macdonald 1988; Lafrance et al. 2004). A stripped outcrop exposing the Tombill-Bankfield fault, and a second larger stripped outcrop, informally named the Portal stripping, showing excellent overprinting relationships between structures and mineralization along the Tombill-Bankfield deformation zone, provide new key information and were mapped in details in 2012 through the current TGI-4 project. They are described below.

Portal stripping

The Portal stripping is a 60 m by 90 m stripped outcrop located along the south limb of the Hard Rock anticline, 300 metres south of the MacLeod-Cockshutt headframe (Figure 1). A feldspar porphyry body takes up more than half of the outcrop (Figure 2). It is pinkish white on outcrop surface, pinkish grey on fresh surface, and it consists of 40 vol. % feldspar phenocryst (1-4 mm in size) and 10 vol. % quartz phenocryst (1-1.5 mm in size) within a fine-grained homogeneous matrix. It contains rare xenoliths of iron formation and altered mafic rock, and it is in intrusive contact with surrounding wacke, iron formation, and green mudstone. The wacke is greenish grey on outcrop and fresh surfaces, and it consists of ≤15 cm thick sandstone beds interlayered with, <1 to 3 cm thick, mudstone beds. Excellent, normal grading, top indicators are observed in the sandstone beds. Iron formation consists of ≤ 20 cm thick, finely laminated, black cherty magnetite beds, interspersed within thickly bedded (≤ 25 cm) wacke similar to that described above. Millimeter scale to 2.5 cm thick, iron formation beds are further associated with laminated to thinly bedded (0.5-2.5 cm) mudstone, varying in color from dark greenish grey on fresh and outcrop surfaces to dark green on outcrop surface. A polymictic pebbly sandstone or conglomerate occupies the southern part of the outcrop. It is brownish light grey to dark grey on outcrop and fresh surfaces, respectively, and it contains strongly deformed, elongate clasts of mafic to intermediate volcanic rocks and sandstone, as well as more spherical clasts of granitic composition. The percentage of clasts is difficult to estimate due to the strong deformation and gradational contacts between clasts and the sandy matrix. Another porphyry, which contains more quartz (10-15 vol. %) and less feldspar (30 vol. %) phenocrysts than the main feldspar porphyry, was emplaced into the green mudstone and wacke with iron formation beds. Numerous, greenish grey to dark brown, gabbroic to ultramafic dikes are roughly parallel to bedding in all rock types. The dikes vary in thickness from a few centimetres to 2 m. They are strongly chloritic, commonly iron-carbonatized and they contains elongate white streaks of carbonatized feldspar(?).

The Portal stripping displays excellent structural overprinting relationships that allow to ascribe ductile structures observed on outcrop to three generations of structures. The oldest generation of structures is represented by an isoclinal synform that occupies the entire width of the wacke panel north of the main feldspar porphyry body (Figure 2). The synform is defined by folded bedding-parallel mafic dikes and by folded sandstone beds that young away from the core of the fold (Figure 3A). The synform youngs downward, thus it has the younging characteristic of a downward-facing synform or synformal anticline. It has a subvertical, west-striking, penetrative axial plane cleavage, and a shallowly (15°-20°), west-plunging, fold axis. The latter is parallel to a strong mineral stretching lineation defined by stretched amygdales and discontinuous dark green chlorite and white carbonatized feldspar in mafic dikes. The cleavage is parallel to the contact between the wacke and the main feldspar porphyry, where it is expressed as a strong sericitic foliation that is penetrative throughout the porphyry. Because early F_1 folds in Geraldton typically lack an axial plane cleavage and because S_2 is the oldest cleavage observed in folded porphyry in the hinge of the F_2 Hard Rock anticline (Lafrance et al. 2004), the downward-facing synform and its axial plane cleavage are interpreted as F_2 and S_2 structures that formed during D_2 north-south shortening across the belt.

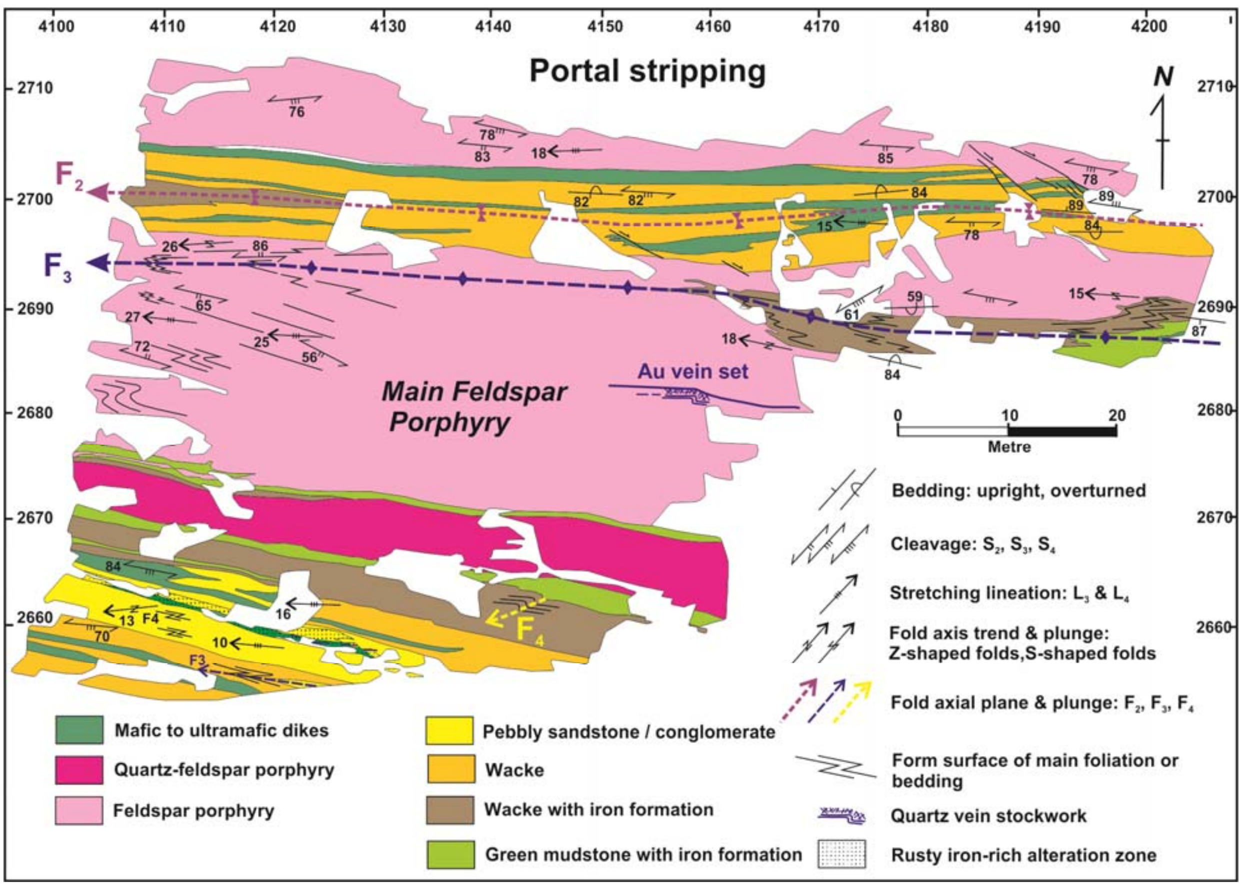

Figure 2: Geological map of the Portal stripping. Location of the map is shown in Figure 1. Co-ordinates represent the last four digits of the Northing 550xxxx and Easting 50xxxx based on the North American Datum 1983 (NAD 83), Zone 16 (Lafrance et al. 2012).

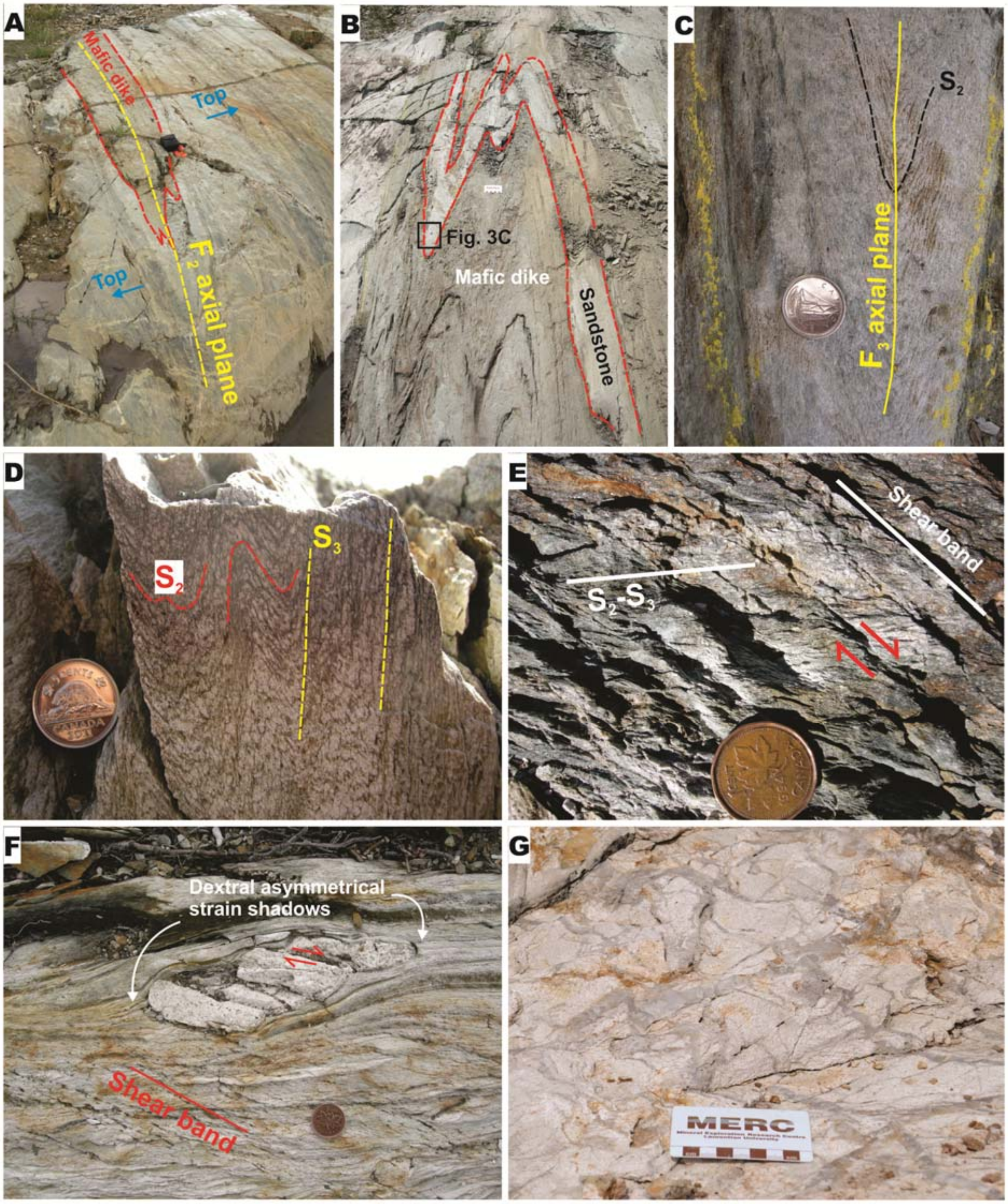

Figure 3: Field photographs of the Portal stripping. A) F_2 synformal anticline. A mafic dike occupies the hinge of the fold. Blue arrows indicate younging direction in wacke. Camera casing, 15 cm in length, for scale. B) S-shaped F_3 fold defined by folded wacke and mafic dikes, north of the main feldspar porphyry body. Photo scale is 9 cm in length. C) Close-up of F_3 fold hinge shown in Figure 3B. S_2 cleavage in wacke is folded by F_3. Coin (18 mm diameter) for scale. D) S_2 cleavage folded by S-shaped F_3 folds along the northern margin of the main feldspar porphyry body. S_3 cleavage is defined by the intensification of S_2 along the long limb of the folds. Coin (20 mm diameter) for scale. E) Penetrative dextral shear bands indicating dextral transcurrent movement, south of the main feldspar porphyry body. Coin (19 mm diameter) for scale. F) Dextral shear bands and dextral asymmetrical strain shadow around granitic clast in conglomerate. Coin (19 mm diameter) for scale. G) Mineralized quartz vein stockwork in the main feldspar porphyry body. Photo scale is 9 cm in length (modified after Lafrance et al. 2012).

The synform is overprinted by a cleavage (S_3) oriented clockwise to bedding on both limbs of the fold (Figure 2). S_3 is a differentiated cleavage defined by chloritic and sericitic foliation planes alternating with 1-2 mm wide white felsic microlithons. It is axial planar to S-shaped F_3 folds in the wacke north of the main porphyry (Figures 3B, C) and, in the porphyry, where the penetrative sericitic S_2 cleavage is folded by F_3 folds, Along the long limbs of asymmetrical F_3 folds, S_3 forms a composite S_2-S_3 fabric expressed by the intensification and decreased spacing of S_2 (Figure 3D). From north to south across the main porphyry body, the asymmetry of F_3 folds changes from S-shaped to M-shaped to Z-shaped and thus the porphyry is folded by a large F_3 fold that has a thin north limb and a thick south limb (Figure 2). The attitude of F_3 folds is similar to that of F_2 folds. Their axial plane is steep and west-striking, and they plunge shallowly to the west (~20º) parallel to a strong stretching lineation represented by rods of presumably recrystallized quartz and feldspar aggregates in the porphyry.

A small, parasitic, F_3 fold on the north limb of the folded porphyry is overprinted by a cleavage (S_4), striking 240º-250º and dipping 80º to the north. S_4 is oriented anticlockwise to bedding and is axial planar to local asymmetrical Z-shaped F_4 folds overprinting S_3. The folds are in turn overprinted by steeply-dipping dextral shear bands striking ~115º to 125º. The orientation of the shear bands is similar to that of dextral shear fractures shown in Figure 2. Shear bands are observed across the main porphyry and wacke, but they become more abundant south of the main porphyry where they form a penetrative dextral slip cleavage (Figure 3E). A bedding- and contact-parallel, composite S_2-S_3 foliation is present in all rock types south of the main porphyry. A shallowly west-plunging stretching lineation, which is defined by rod-like elongate pebbles in conglomerate, lies along the composite foliation plane. The intersection lineation between the dextral shear bands and composite S_2-S_3 foliation is roughly perpendicular to the shallowly-plunging stretching lineation, which is consistent with the formation of these structures during dextral transcurrent shear. On horizontal surface, strong granitic pebbles are surrounded by dextral asymmetrical strain shadows. The clasts locally contain NW-SE oriented steeply dipping extensional quartz veinlets and weak elongate volcanic clasts are folded by Z-shaped F_4 folds, further suggesting dextral transcurrent shear (Figure 3F). Although these structures occur throughout the Portal stripping, they are more abundant or pronounced in the southern part of the stripping where dextral transcurrent shear was more intense. F_4 and S_4 correspond to F_3' and S_3' of Lafrance et al. (2004), which are interpreted as late structures that formed during a progressive D_3 dextral transpressional event that began with the formation of F_3 folds, a regional S_3 cleavage, and dextral transcurrent shear zones.

A set of milky fault-fill white quartz veins with minor ankerite yielded high gold values (Premier Gold Mines Ltd. pers. com.) The veins were emplaced in the main porphyry body on the south limb of the large F_3 fold (Figure 2). They strike east (100°), dip south (60°), and they are up to 10 cm thick. They are associated with a stockwork of smaller quartz veins and surrounded by silicified porphyry containing minor pyrite (Figure 3G). The quartz veins are folded by a Z-shaped F_3 fold that is parasitic to the large F_3 fold, they are transposed and locally boudinaged suggesting either early- or pre-D_3 emplacement of the gold-bearing veins.

Tombill-Bankfield Fault stripping

The Tombill-Bankfield fault is described as a zone of intense shearing, brecciation, silicification, and carbonatization (Pye 1952; Horwood and Pye 1955). It was thought to be a major break that influenced the location of most deposits in Geraldton (Pye 1952). This recently led Premier Gold Mines Ltd to excavate 3-4 m of overburden to expose bedrock where a drill hole intersected black smoky quartz veins along the trace of the fault. This new stripping is the best known exposure of the fault at surface, but it will be reburied during the coming year.

The fault occurs at the contact between diorite to the south and sandstone to the north (Figure 4). The sandstone is interleaved with diorite, mafic pillowed flows, and a fine-grained, synvolcanic, mafic dike. Diorite is greenish dark grey on outcrop and fresh surfaces. It consists of ~45% chloritized green amphibole, up to 1 cm in size, surrounded by greenish white feldspar. Epidote-quartz-amphibole patches and veins occur throughout the rock and are cut by late quartz-iron carbonate veins. Local tourmaline-rich quartz veins and breccias are present. Sandstone varies in color and composition from a more sericitic, greenish light grey rock with bed thicknesses of 2 to 10 cm and grain size of 1-2 mm, to a more chloritic, brownish dark grey, interlayered sandstone-mudstone with bed thicknesses of 2-5 cm. Mafic pillowed flow consists of dark green, aphyric pillows with thin, ~1 cm thick, selvages (Figure 5A). The synvolcanic dike is dark green, aphyric and massive. It is in sharp contact with the diorite and mafic pillowed flow. The mafic pillowed flow and synvolcanic dike are cut by multiple epidote-quartz veins which are in turn transected by quartz-iron carbonate-tourmaline veins.

The diorite has a strong differentiated foliation (S_2) defined by feldspar-rich, felsic bands, alternating with amphibole –rich, mafic bands (average thickness of 3-5 mm). S_2 strikes east (~100°) and dips steeply (70°-85°) to the south. It is folded by Z-shaped F_3 folds associated with an axial plane S_3 cleavage defined by chlorite. S_3 is oriented anticlockwise to S_2; it strikes east-northeast (70°-85°) and dips steeply (70°-85°) to the south. S_3 becomes more intense and closely spaced in narrow shear zones (<50 cm thick) surrounding less deformed, metre wide, lozenges of diorite. The shear zones contain a shallowly west-plunging (~15°), chloritic, mineral lineation, similar in orientation to F_3 fold axes. Dextral shear bands, striking ~°120 or ~°300 and dipping steeply (80°-85°) to the south or north, and Z-shaped drag folds defined by folded quartz-iron carbonate veins, are present along most shear zones, suggesting dextral transcurrent shear. Pillows in the mafic pillowed flow are flattened parallel to S_2. The strain appears to increase in intensity within sandstone and mudstone where S_2 is oriented parallel to bedding and S_3 is oriented anticlockwise to S_2 as observed in the diorite. Similar dextral shear sense indicators, that is, shear bands and drag folds, are developed in sheared sandstone/mudstone and mafic pillowed flow but, in addition, spectacular dextral asymmetrical strain shadows are present around pillow fragments (Figure 5B).

Black smoky fault-fill quartz veins occur along the fault. The fault is oriented parallel to S_2 and so it formed either during or after D_2. The veins are individually 1-15 cm thick and collectively ~1 m thick, and they strike 90º-105º and dip 75º-85ºS parallel to the fault. They are cut by multiple, mm-thick, milky white, quartz veins, filling fractures that are perpendicular to the margins of the black smoky quartz veins and that span the width of those veins. A 1.5 m-thick, bleached (light grey), alteration halo surrounds the black smoky quartz veins. The veins were broken up and brecciated (Figure 5C), and an anticlockwise S_3 cleavage formed in the alteration halo, during D_3 dextral shear reactivation of the fault. Pyrite and chalcopyrite(?) occupy dextral shear bands that have a strike of 125º-140º and a dip of ~70º to the south (Figure 5D), similar to the orientation of shear bands associated with narrow dextral shear zones north and south of the fault. Thus, the smoky quartz veins were emplaced either during D_2 or early during D_3, and sulphide mineralization was remobilized into shear bands during D_3 dextral shear.

Grab samples of of the veins yielded low gold values so no further exploration work is planned for this stripping and fault (Premier Gold Mines Ltd., pers. com.).

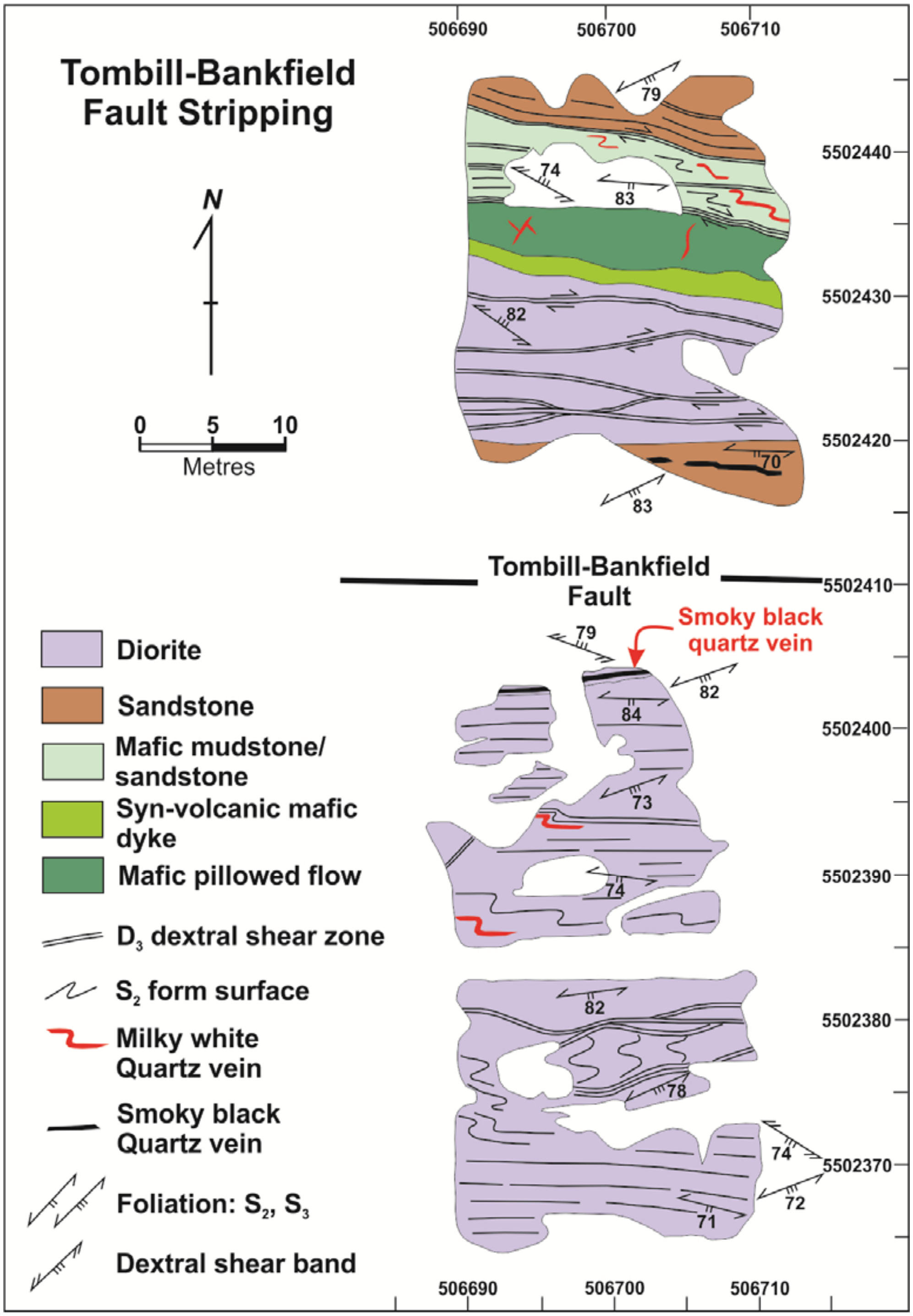

Figure 4: Geological map of the Tombill-Bankfield fault stripping. Location of the map is shown in Figure 1. Co-ordinates are based on the North American Datum 1983 (NAD 83), Zone 16. Modified after Lafrance et al. 2012.

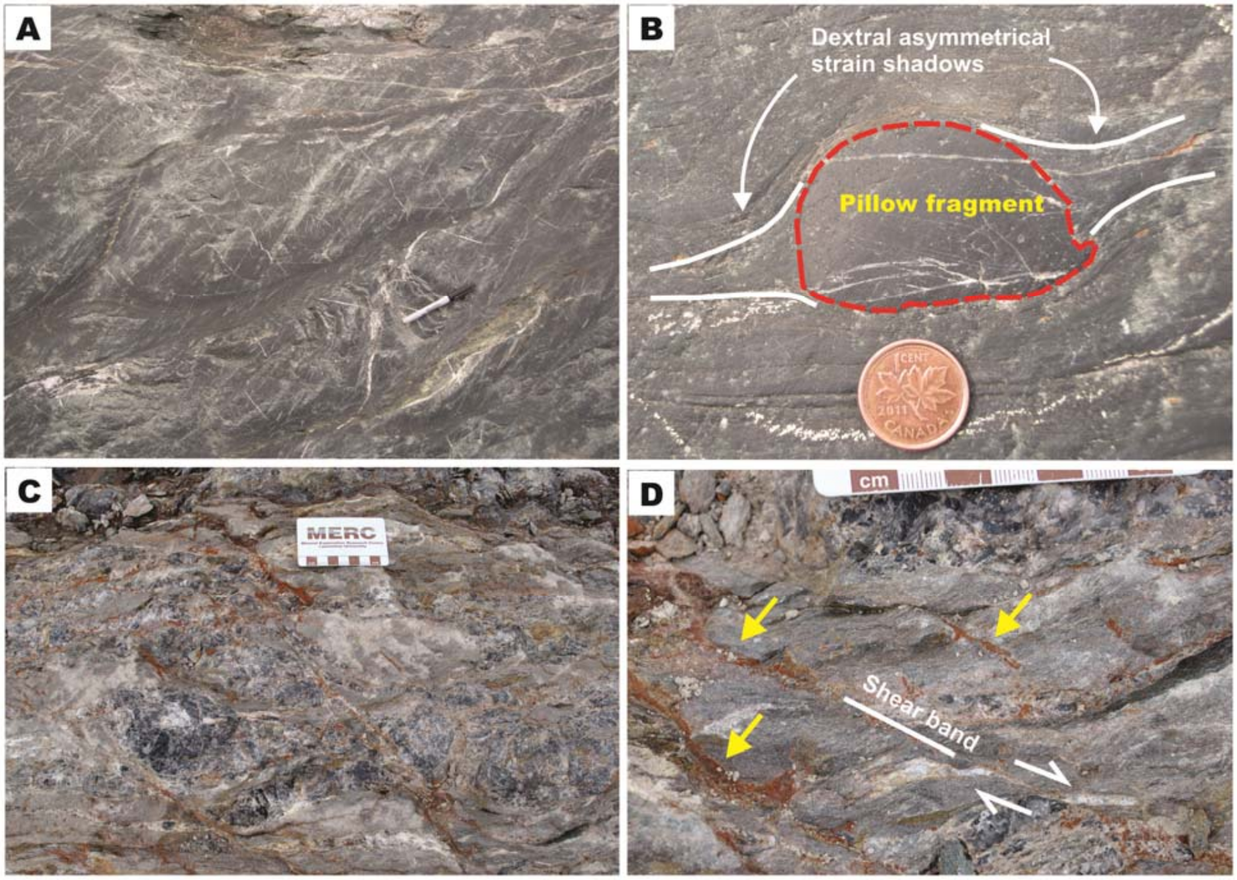

Figure 5: Field photographs of the Tombill-Bankfield stripping. A) Pillow in mafic pillowed flow. Pencil is 10 cm in length. B) Dextral asymmetrical strain shadows around pillow fragment. Coin (19 mm diameter) for scale. C) Fractured and broken-up smoky black quartz vein along the Tombill-Bankfield fault. Photo scale is 9 cm in length. D) Sulphide mineralization (indicated by yellow arrows) was emplaced along dextral shear bands during D_3 (Lafrance et al. 2012).

Conclusions

Mineralization at the Portal stripping consists of auriferous quartz veins that are pre- or early-D_3. The ore zones are deformed and folded, which are important controls on their geometry and distribution. On the other hand, at the Tombill-Bankfield Fault stripping, sulphide mineralization emplaced in or remobilized into shear bands syn-D_3 and fault-fill veins are either syn-D_2 or early-D_3. Thus, there are at least two mineralizing events in the Geraldton area. Ore zones may have formed during more than one mineralization event or, alternatively, they may have formed during one mineralization event and were subsequently upgraded during a subsequent event.

Preliminary observations on gold mineralized zones in the Geraldton area

Close to 2500 m of core from four drill holes was logged during the 2012 summer field season. Three of the four drill holes (MM179, MM179C, MM179D) intersected the F Zone whereas the fourth drill hole (MM106D) intersected the North Zone. The two zones represent the bulk of the resources delineated in Geraldton. MM179C and MM179D are wedged drill holes from drill hole MM179. MM106D is a wedged drill hole from drill hole MM106. These drill holes were recommended for detailed study by geologists of Premier Gold Mines Ltd. because of their high gold intercepts and the key information and features about the mineralization styles. Premier Gold Mines provided access to their drill hole database, which include gold assay results and important information on rock type and alteration.

The F Zone and North Zone are located on the north limb of the Hard Rock anticline. Different styles of alteration and gold mineralization are associated with the two zones. They reflect the rock types hosting mineralization, and they are subdivided into porphyry-, sandstone-, sandstone-minor iron formation, and iron formation-hosted styles of gold mineralization and alteration. The most important observations from each drill hole are summarized below. The complete drill logs are in Appendix A.

MM179

An altered quartz-feldspar porphyry intrusion was intersected at down hole depths of 663.6 m to 737.7 m. The intrusion is thoroughly altered and mineralized. The mineralization is associated with quartz-ankerite-calcite veins with strongly silicified wallrocks that contain up to 5 % pyrite ± arsenopyrite ± pyrrhotite. Disseminated pyrite is present throughout the intrusion but pyrite is coarser grained within higher gold grade intervals.

At depths of 744 m to 745.5 m, a mineralized 1.5 m interval is present within sandstone interlayered with mudstone and minor iron formation. The interval contains 5 % disseminated pyrite ± arsenopyrite ± pyrrhotite in chlorite-sericite alteration haloes surrounding quartz-carbonate (ankerite+calcite) veins.

The F Zone was intersected at a down hole depth of 774 m within interlayered mudstone-sandstone. The zone is only 1.5 m thick. The alteration and sulphide minerals are similar to those described above and consist of sericitic and carbonate-rich alteration halo with 2-3 % pyrite-pyrrhotite-arsenopyrite surrounding quartz-ankerite veins.

A different style of alteration and mineralization is present in green mudstone interlayered with iron formation, intersected at depths of 819.1 m to 845.4 m. Massive pyrite replacement zones are associated with quartz-ankerite-minor calcite-pyrite veins with chlorite selvages. No pyrrhotite or arsenopyrite is present.

MM179C

The first mineralized interval is at down hole depths of 603 m to 606 m, where it is hosted by interlayered mudstone, sandstone, and minor iron formation. It consists of quartz-ankerite ± calcite veins surrounded by alteration halo of sericite ± chlorite in mudstone and carbonate (calcite, ankerite) in sandstone. Chalcopyrite-pyrite as well as minor arsenopyrite-pyrrhotite are present within both the veins and alteration haloes. The same interlayered mudstone-sandstone-iron formation hosts another mineralized zone (616.5-635 m) with similar features, called the SP zone or South Porphyry zone. In addition to the alteration features described above, interlayered iron formation beds are partially replaced by pyrrhotite-pyrite-chalcopyrite-arsenopyrite. This replacement texture appears to be associated with quartz-carbonate veins. Late fractures filled with coarse grained pyrite-pyrrhotite and chlorite cut across the veins and massive sulphide replacement bands.

From 655 m to 666.4 m, iron formation beds interlayered with mudstone and sandstone are replaced by pyrrhotite in turn overgrown by semi-massive arsenopyrite±pyrite (665-666 m). The sulphides are associated with calcite alteration of the host rocks and with quartz-carbonate veins.

The F Zone is intersected at a depth of 670.5 m. It drastically increases in thickness from 1.5 m in previous drill hole MM179 to 32.5 m in this drill hole. The F Zone straddles several rock types so the style of alteration and mineralization changes across the zone. From 670.5 m to 675.5 m, the F Zone is hosted by a quartz-feldspar porphyry intrusion, strongly altered to carbonate and containing 2-3 %, coarse grained, disseminated pyrite-arsenopyrite associated with quartz-carbonate veins. The veins make up 2-3% of the rock and are surrounded by strong calcite-chlorite-sericite selvages. From 675.5 m to 680.4 m, the F Zone mineralization is associated with quartz-ankerite veins with strong sericite alteration halo within interlayered mudstone and sandstone. Pyrite, arsenopyrite, and free gold are present in the veins. From 680.4 m to 689.5 m, the F Zone mineralization consists of semi-massive sulphide ore with up to 70% pyrite and arsenopyrite. The distribution of the sulphides is spatially zoned within the alteration haloes surrounding quartz-ankerite veins. Sulphides are coarser and pyrite is more abundant close to the veins whereas the sulphides become finer-grained and arsenopyrite is more abundant away from the veins. From 689.5 m to 692.4 m, the F Zone is in a quartz-feldspar porphyry intrusion with alteration and mineralization similar to that described above, and from 692.4 to 712 m, the F zone is hosted by interlayered mudstone-sandstone. The abundance of quartz-ankerite veins with sericite-arsenopyrite-pyrite halo decreases towards the end of this interval. Late pyrrhotite-arsenopyrite-chalcopyrite stringers cut across black mudstone horizons, and pyrite-pyrrhotite-infilled fractures cut across the quartz-ankerite veins.

The F Zone reappears between the depths of 717.6 m to 725.6 m after a barren interval of roughly 5 m in thickness. Interlayered mudstone-sandstone contain 40 % sericite-ankerite ± chlorite in alteration halo around quartz-ankerite±calcite veins. The veins increase in abundance from 5-7% of the rock in the upper part of the interval to 40 % below 723 m.

From 729.4 m to 731 m, quartz-ankerite veins with pyrite-arsenopyrite-pyrrhotite alteration halo are present in interlayered mudstone-sandstone. Pyrrhotite is replaced by coarse-grained arsenopyrite within the alteration halo. A younger set of chlorite-pyrrhotite veins cut across the quartz-ankerite veins.

MM179D

The F Zone was intersected at a depth of 656 m. It is 3 m thick and it consists of quartz-ankerite ± pyrrhotite with chlorite-biotite-arsenopyrite selvages in interlayered mudstone-silttone-sandstone. Other mineralized intervals in the same host rocks were intersected at depths of 648.5 m to 659 m, and 731.5 m to 737.5 m. They are characterized by quartz-ankerite ± calcite±chlorite veins with minor pyrite-chalcopyrite-pyrrhotite. The veins are surrounded by sericite-ankerite-pyrite and chlorite-biotite±sericite±calcite±arsenopyrite alteration haloes.

Magnetite-rich iron formation beds interlayered with mudstone and sandstone (613-614.7 m) are replaced by coarse grained pyrite-arsenopyrite-pyrrhotite associated with 2-3 % of quartz-calcite veins surrounded by strong chlorite alteration halo.

Reddish black-black iron formation interlayered with mudstone hosts two mineralized intervals within the so-called K zones (783.7-784.9; 787.4-791 m). The mineralized intervals are characterized by brownish yellow, sericite-chlorite-carbonate alteration surrounding quartz-carbonate veins. Disseminated pyrite (2-3 %) occurs in the alteration halo, the veins and as sulphide replacement of iron formation beds.

MM106D

The best mineralized intervals are associated with iron formation at depths of 769 m to 771.3 m and 779.2 m to 822.2 m. Iron formation is black and magnetite-rich and/or dark red and composed of cherty jasper beds. The mineralized intervals consist of semi-massive pyrite±arsenopyrite±pyrrhotite replacement zones surrounding quartz-ankerite±chlorite veins.

Mineralization occurs in mafic dikes (619.2-656.7 m) intercalated with quartz-feldspar porphyry (656.7-680.4 m). Quartz-ankerite±pyrite±tourmaline veins are surrounded by chlorite-sericite-pyrite-fuchsite(?) halo in mafic dikes and by intense sericite-ankerite-pyrite alteration halo in porphyry.

Quartz-ankerite veins with sericite alteration haloes are present with interbedded sandstone and mudstone. 2-3%, disseminated pyrite-arsenopyrite±pyrrhotite are present in both the veins and their alteration haloes.

Synthesis

The **F Zone** comprises two main styles of mineralization: sandstone-hosted and porphyry-hosted mineralization and alteration. Sandstone-hosted mineralization is characterized by quartz-ankerite±calcite veins with chlorite selvages. The veins have a strong yellow-brown sericite-(chlorite?) alteration halo in mudstone and a strong carbonate-sericite alteration halo in sandstone. Pyrite +/- arsenopyrite +/- pyrrhotite +/- chalcopyrite are present in the veins and in their alteration halo. Pyrite and arsenopyrite are commonly coarse-grained and rare free gold is locally present in the veins. The veins are typically strongly folded and commonly transposed and boudinaged parallel to a bedding-parallel foliation. Typical sediment-hosted F Zone style mineralization is shown on Figure 6a.

Porphyry-hosted mineralization is characterized by strong carbonate (calcite certainly, ankerite?) -sericite ± chlorite alteration halo surrounding deformed quartz-ankerite veins. Gold grades are lower within the porphyry relative to the interlayered mudstone-sandstone but alteration is more pervasive and gold is more evenly distributed.

The **North Zone** is hosted by magnetite-rich iron formation interlayered with grey to green mudstone-sandstone. Gold-bearing semi-massive sulphides have replaced beds in iron formation and possibly interlayered sandstone and mudstone. The sulphides include pyrite +/- arsenopyrite +/- pyrrhotite +/- chalcopyrite. The sulphides surround strongly deformed quartz-ankerite±chlorite veins with chlorite and/or calcite haloes. Pyrite and arsenopyrite overgrow earlier sulphide minerals (pyrite-pyrrhotite), and arsenopyrite is in turn locally overgrown by later coarse grained pyrite. Variations of North Zone style alteration and mineralization are shown on Figure 6/b-f.

Iron formation-hosted mineralization is commonly surrounded by sandstone-hosted mineralization. The latter consists of gold-bearing quartz-ankerite veins with strong sericite-carbonate ± chlorite alteration halo, alternating with semi-massive sulphide (arsenopyrite-pyrite) replacement zones roughly concordant to bedding and foliation. Sulphide minerals within the alteration haloes are typically zoned with pyrite adjacent to the veins and arsenopyrite more distal to the veins.

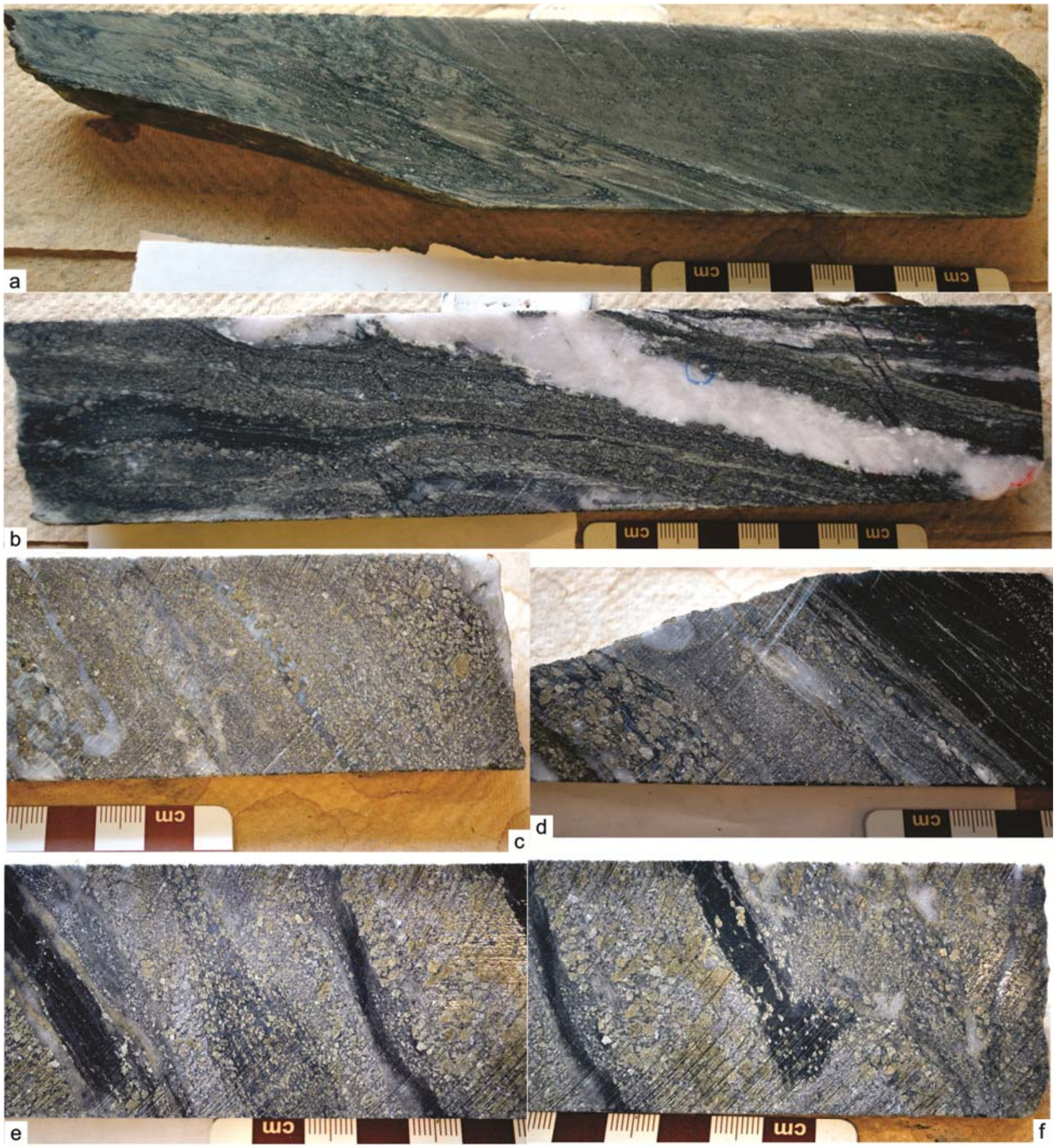

Figure 6. **a**, *BGBST2012_152*: MM179C 677.5-677.9 m Strongly sericitized rock characteristic of the F Zone. Semi-massive sulphide replacement mineralization typically associated with quartz-carbonate veins: **b**, *BGBST2012_154: MM179C 681.27-681.50 m;* **c-d**, *BGBST2012_300: MM106D 785.33-786 m;* **e-f**, *BGBST2012_304: MM106D 797.2-797.76 m* .

Petrography

The following observations are from four thin sections that are representative of the F Zone and North Zone.

BGBST2012_152

The thin section is from interval 677.5 m to 677.7 m in drill hole MM179C drill hole. It represents the F zone. The host rock is interlayered mudstone-sandstone.

Texture: The rock has an equigranular granoblastic texture with a foliation defined by sericite. Sulphide-bearing quartz-carbonate veins (Figure 7a) are boudinaged and the foliation wraps around the veins. The rock consists of 60% sericite, 25 % carbonate, 10 % quartz and 5 % opaque grains where it is most sericitized, and it consists of 50 % carbonate, 30 % sericite, 13 % quartz and 7 % opaque minerals where it is least sericitized. Slightly folded veins of quartz-carbonate veins include magnetite, pyrite, arsenopyrite, and chalcopyrite (Figure 7b, c). Disseminated magnetite and chalcopyrite are present in the altered rock and magnetite also occurs as inclusions in pyrite and arsenopyrite in the veins. Pyrrhotite occurs with magnetite and chalcopyrite as inclusions in pyrite.

BGBST2012_154

The thin section is from 681.27-681.5 m in drill hole MM179C. It is from the North Zone. The host rock is an interlayered mudstone-siltstone.

The thin section is subdivided into 7 sections representing veins, and alternating strongly altered and less altered mineralized layers.

1. This section is a quartz-carbonate vein surrounded by strong sericite and minor chlorite defining a foliation. Pyrite is elongate parallel to foliation. Magnetite occurs as inclusions in pyrite and as dissemination in the altered rock. Trace native gold fills fractures in pyrite (Figure 7d) and occurs as separate grains in the altered rock.
2. These two sections are strongly mineralized and they consist of 50 % opaque minerals, 30 % carbonate, 10 % sericite and 10 % quartz. Quartz and carbonate occur as veins and

as groundmass. Sericite alteration is stronger adjacent to the veins where it is associated with opaque minerals, including pyrite, minor magnetite and gold.

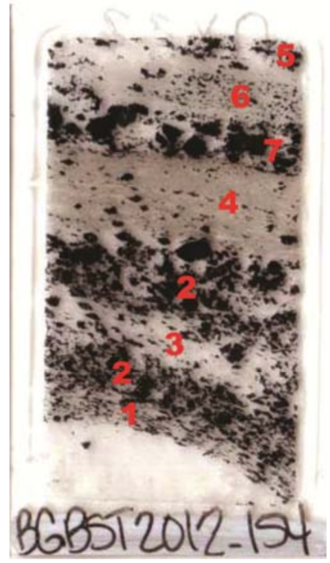

3. Less mineralized section is similar to section 1 but it contains more quartz and carbonate, as well as sericite and opaque minerals in equal proportion
4. Less mineralized section comprises 40 % fine grained quartz, 35 % chlorite, 20 % carbonate and 5 % opaque minerals (Figure 7e). The latter consists of 2 % arsenopyrite and 2 % pyrite with trace inclusions of chalcopyrite, pyrrhotite and magnetite in pyrite grains.
5. This section comprises 45 % fine grained quartz, 45 % carbonate, 5-10 % opaque minerals (arsenopyrite, pyrite, magnetite) as well as minor chlorite and sericite defining a weak foliation (Figure 7f).
6. Strongly mineralized section consists of coarse-grained pyrite (14%) and arsenopyrite (5%) with fine-grained chalcopyrite (1%) and magnetite surrounded by a groundmass matrix of quartz (50%), carbonate (25 %) and sericite (5 %).
7. Strongly mineralized section similar to section 2 consists of 30 % pyrite, 18 % arsenopyrite, 1 % chalcopyrite and minor magnetite, surrounded by a quartz, carbonate, and sericite matrix.

In general, pyrite grains are anhedral, microfractured, and elongate parallel to foliation (Figure 8a). Arsenopyrite appears to overgrow pyrite. Pyrite and arsenopyrite were emplaced prior to or during deformation whereas gold may be coeval with or later that the sulphide minerals.

BGBST2012_300B

The thin section is from the interval 785.33 m -786 m in drillhole MM106D. It represents strongly sulphide-rich layers from the North Zone.

Two sections are observed:

1. The first section contains 40-45 % opaque minerals, 30 % quartz, 30 % carbonate, minor sericite and trace chlorite. It likely represents a recrystallized vein. The mineralization

consists of arsenopyrite (24 %) intergrown with anhedral, coarser grained pyrite (19 %) (Figure 8b). Minor pyrrhotite, chalcopyrite and magnetite are also present. Gold occurs as inclusions and fracture-filling in pyrite (Figure 8c).

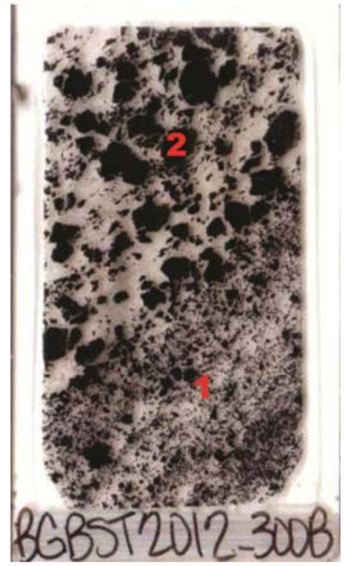

2. The second section represents presumably the strongly sericitized wall rock of the vein in section 1. It consists of sericite, carbonate, quartz, sulphide and lesser biotite and chlorite. Sericite defines a foliation overprinted by a crenulations cleavage (Figure 8d) and kink bands. Lath-shaped arsenopyrite occurs along and are elongated parallel to the foliation and crenulations cleavage (Figure 8e). Sulphide grains underwent cataclasis parallel to foliation. Associated with quartz-carbonate veins are coarse-grained, subhedral, arsenopyrite and pyrite, which mutually overgrow each other suggesting that they are coeval. Trace pyrrhotite, arsenopyrite and native gold occur as inclusions in pyrite.

BGBST2012_304

The thin section is from interval 797.2-797.76 m in drill hole MM106D drillhole. It is from the North Zone.

It is subdivided in 3 sections:

1. The first section consists of 35 % chlorite, 20 % carbonate, 15 % sericite, 15 % opaque minerals, and 5-5 % biotite and quartz (Figure 9a). Magnetite (5 %) occurs in a band parallel to foliation (Figure 9b) and is overgrown by pyrrhotite (2 %), which is in turn overgrown by coarse grained pyrite (7 %), arsenopyrite (1 %) and chalcopyrite (trace). Magnetite and chalcopyrite also occur as inclusions in pyrite. Chlorite defines a foliation that wraps around the sulphide grains. Calcite and quartz crystallized in strain shadows surrounding magnetite grains.

2a. It consists of 40 % carbonate, 30 % sericite, 25 % quartz, 2 % pyrite, 1 % pyrrhotite, arsenopyrite, and trace magnetite. Pyrite and arsenopyrite overgrow magnetite. Magnetite, pyrrhotite, and chalcopyrite occur as fine inclusions in pyrite whereas arsenopyrite contains pyrrhotite and magnetite inclusions only (Figure 9c)

2b. Folded finer-grained section consists of 40 % opaque minerals, 30 % carbonate, 20 % sericite and 10 % quartz (Figure 9d). Magnetite and pyrrhotite were found as inclusions in coarse grained pyrite. Native gold is present as inclusions in pyrite (Figure 9e).

3. The third section represents a vein composed of 50 % carbonate (inequigranular, interlobate), 35 % carbonate (inequigranular, interlobate), 5 % feldspar (aggregate of coarse feldspar; sericitized), 5 % sericite, 3% anhedral pyrite and 2 % euhedral arsenopyrite.

Summary

The F Zone is characterized by strong sericite and carbonate alteration. It comprises 5-10 % opaque minerals including pyrite>arsenopyrite, lesser magnetite and chalcopyrite, and trace pyrrhotite. Magnetite, pyrrhotite and chalcopyrite occur as inclusions in coarse grained, anhedral-subhedral pyrite and arsenopyrite.

The North Zone is characterized by semi-massive sulphide replacement of the host rock surrounded with variably intense carbonate and sericite alteration. The emplacement of the sulphide is associated with quartz-carbonate veins. Sulphide minerals typically represent more than 50 % of the rock and consist mainly of pyrite with slightly less abundant arsenopyrite and lesser pyrrhotite, chalcopyrite, magnetite and native gold. Gold mostly occur as inclusions or in fractures in pyrite as well as occasionally as unique specks. Fine grained, disseminated, euhedral arsenopyrite occurs along foliation and crenulations cleavage in sericite-rich bands.

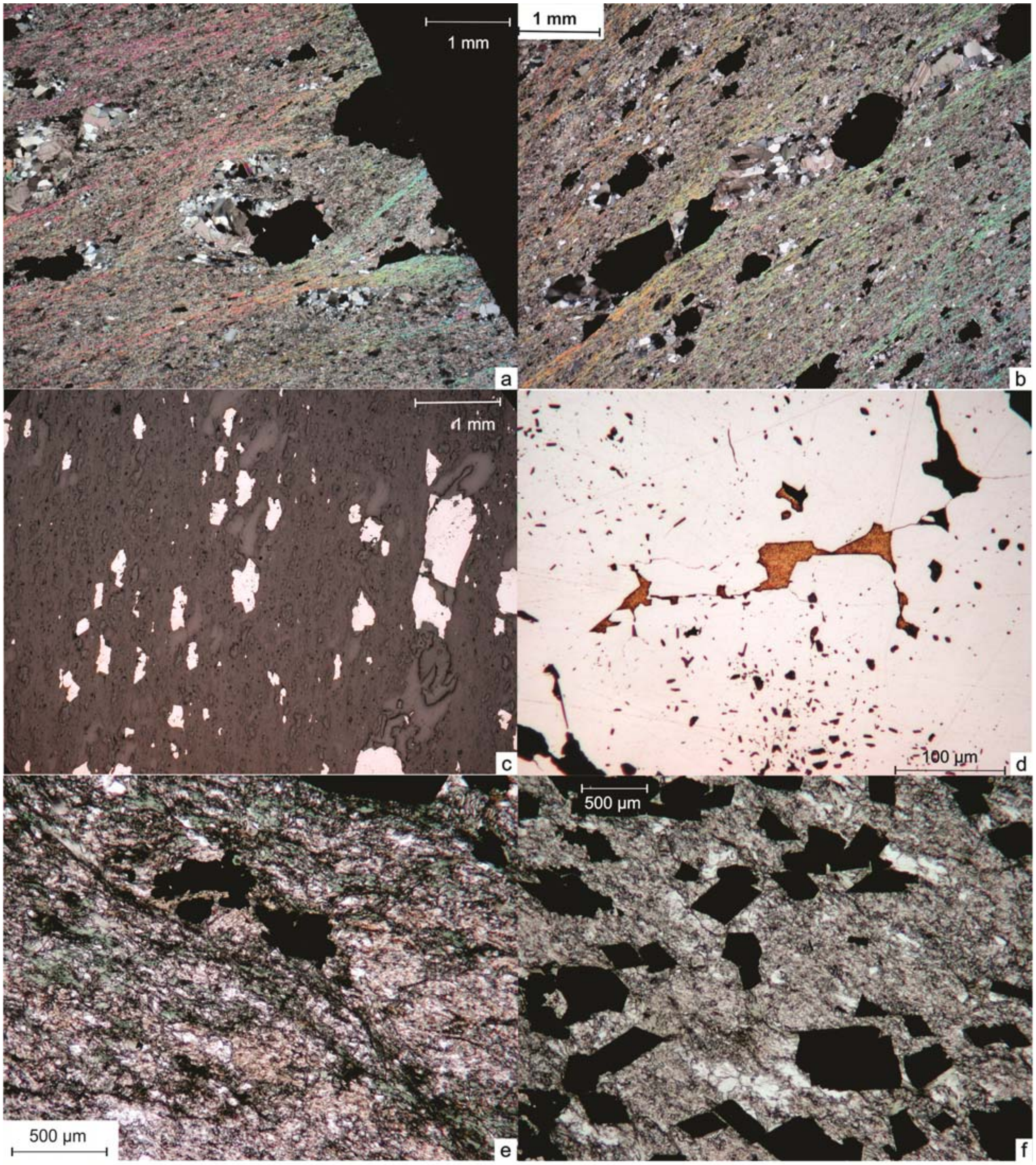

Figure 7. *BGBST2012_152*: **a**, Quartz-carbonate-sulphide vein is wrapped around by the foliation defined by sericite. **b**, A general overview of the texture in this strongly sericitized rock. Slightly folded quartz-carbonate-opaque (pyrite-arsenopyrite-magnetite). Strong foliation wraps around opaque grains. **c**, Sulphide grains oriented parallel to folitation. The sulphide grains, generally pyrite and to a lesser degree arsenopyrite appear to be anhedral-subhedral. *BGBST2012_154:* **d**, Specks of native gold in large, resorbed pyrite. **e**, Overview of the fourth subsection representing a less mineralized interval. **f**, General overview of the fifth subsection representing a moderately mineralized zone.

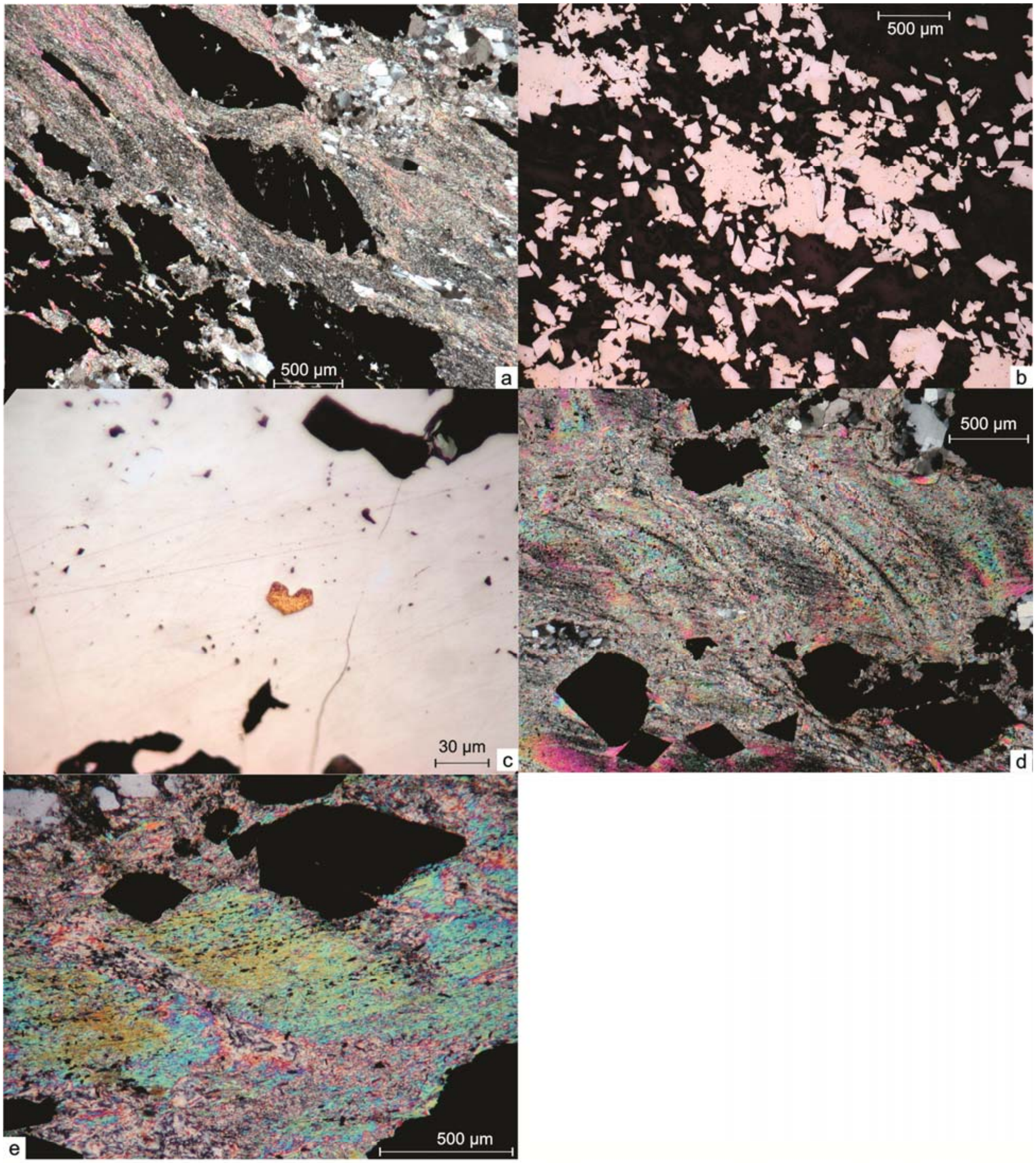

Figure 8. *BGBST2012_154*: **a**, Subhedral pyrite grain broken up by shear fractures and wrapped around by sericite-defined foliation. Elongated parallel to foliation. *BGBST2012_300B*: **b**, Overview photograph of the first, arsenopyrite-rich zone showing overgrowing anhedral pyrite and subhedral arsenopyrite. **c**, A speck of native gold in large, resorbed pyrite grain. **d**, Overview photograph of crenulation clevage in strongly sericitized wall rock. **e**, Recrystallized sericite in shear zones with abundant disseminated, lath-shaped arsenopyrite emplaced in the crenulation clevage and oriented along the older foliation.

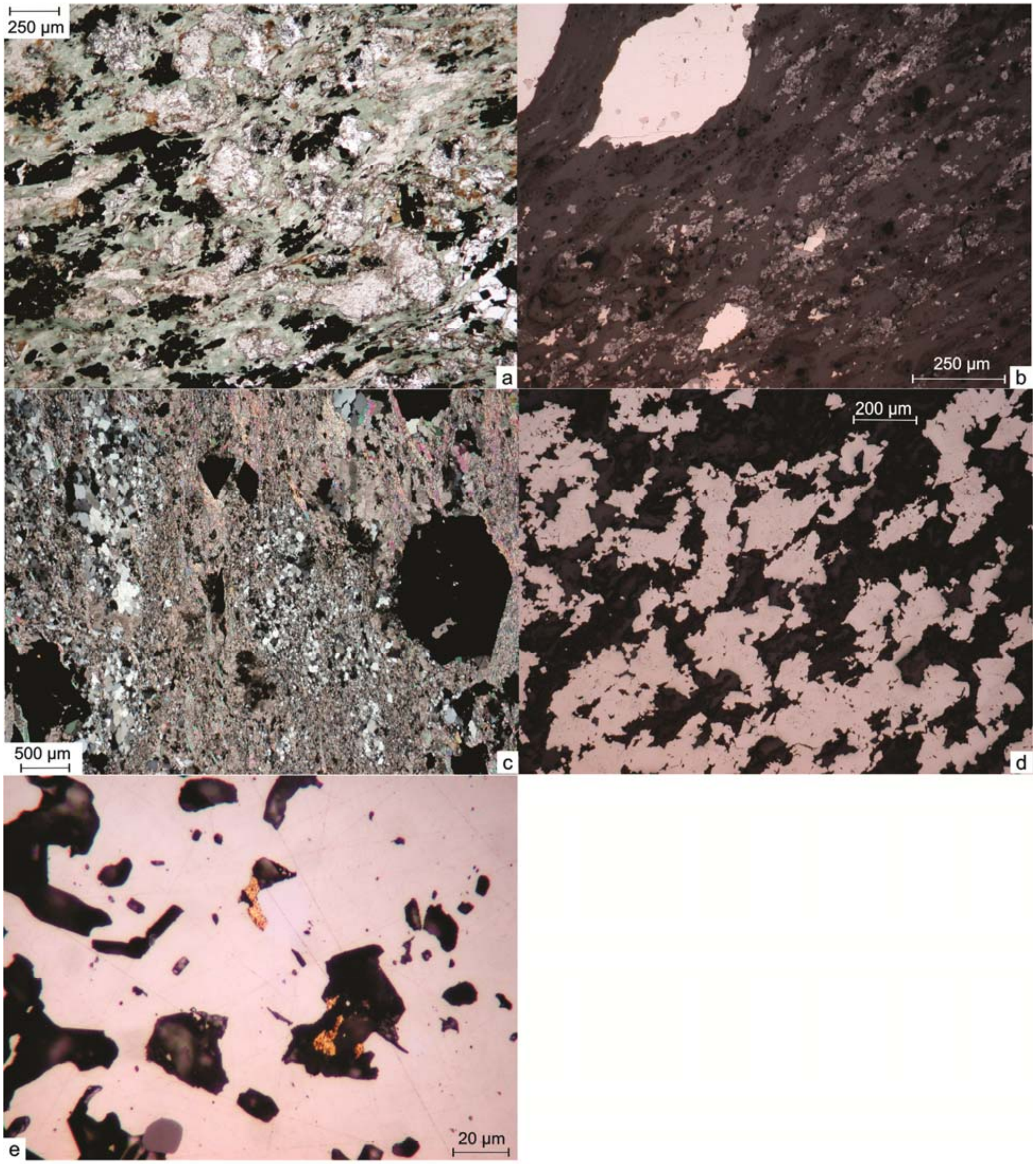

Figure 9. *BGBST2012_304*: **a**, Average overview photograph showing possibly the least altered host rock in the first subsection **b**, Magnetite appears in a well-definable zone (first subsection) and is overprinted by pyrrhotite which is overprinted by coarse grained pyrite and arsenopyrite. **c**, An overview photograph showing the less mineralized quartz-rich zone (2a) that surrounds the folded, strongly mineralized semi-massive sulphide band. **d**, Overview photograph of semi-massive pyrite mineralization in 2b zone. **e**, Specks of native gold in large, resorbed pyrite grain.

Geochemistry

113 samples out of 262 collected samples were selected for geochemical analysis. Care was taken to select samples without veins to minimize dilution due to the introduction of vein material.105 samples were analysed for major element oxides (XRF), CO_2 (Coulometry), $S_{(total)}$ (Leco), FeO (Titration), As-Bi-Se-Sb-Te (Aqua regia ICP-MS) and 46 trace elements (Li meta/tetraborate fusion ICP-MS; ICP-MS following four-acid digestion for chalcophile elements) at Activation Laboratories in Ancaster, Ontario. Additional analyses were done by fire assay for Au, Ag, and by ICP following aqua regia dissolution for Cu, Zn, Pb, Ni if they exceeded the ICP-MS upper detection limits for those elements. Another 8 samples were analyzed for their major element oxide and trace element composition only.

The analyses were done to establish the geochemical footprint of the mineralized zones. Preliminary results are presented below as binary diagrams with Au, pathfinder trace metals, alkali oxides, and alteration indexes along the x- and y-axes.

Au versus total S: Samples are divided according to rock type (Fig. 10). Sulphur shows good correlation with gold regardless of the host rock.

Au versus SiO_2: SiO_2 shows a well-defined negative correlation with Au suggesting significant change in the silica content compared to the other elements accompanying the mineralization process (Fig. 11).

Au versus CO_2 plot shows no correlation with gold suggesting that carbonation is not closely associated with the gold mineralization. It is likely a more extended process than the mineralization itself (Fig. 12).

Au versus $SiO_2/(CO_2+S)$ plot suggests enrichment in gold with increasing sulphidation (-carbonation) and decreasing relative silica content (Fig. 13).

K_2O versus Na_2O: There is generally a reverse correlation between K_2O and Na_2O (Fig. 14) for most rock types in the North Zone and F Zone likely due to replacement of feldspars during sericitization. This correlation is very strong within porphyry in the F zone and in sandstone in the North Zone, but is lacking in sandstone within the F Zone.

Au versus Na_2O: Na value is relatively low in every strongly sulphidized samples with high gold value suggesting Na depletion (presumably during sericitization) associated with the North Zone style mineralization process (Fig. 15).

Au versus pathfinder trace metals: Binary plots of Au versus Te, Ag, As, Bi, Sb, W show poor correlations between Au and these elements. As and Te values correlate positively with Au values and samples with higher Au values generally have higher As and Te values (Fig. 16). However, some samples with high Au values have low As and Te values and others with low Au values have high As and Te values. Arsenic shows moderate correlation with Au suggesting that part of the mineralization is associated with As enrichment, but the spread of the data also suggests gold mineralization occurring without strong As enrichment (Fig. 17.)

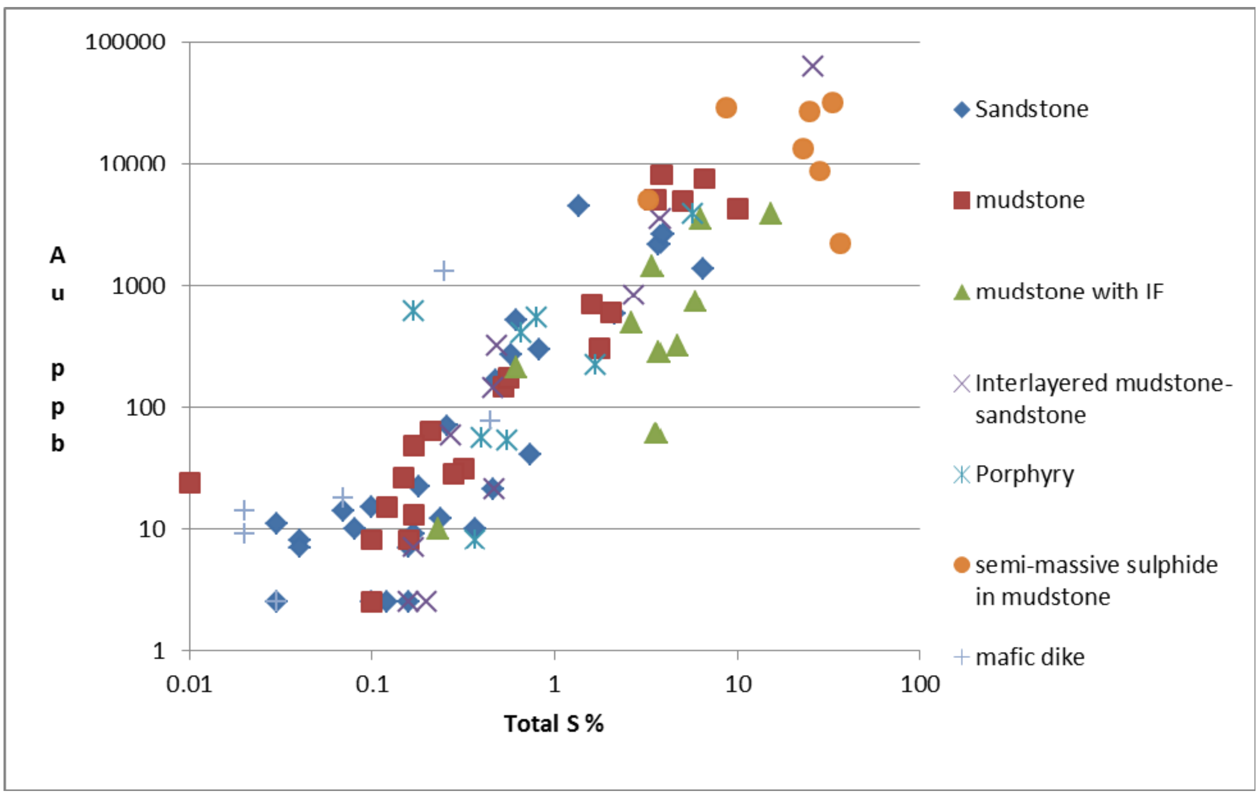

Figure 10: Au versus total S binary diagram

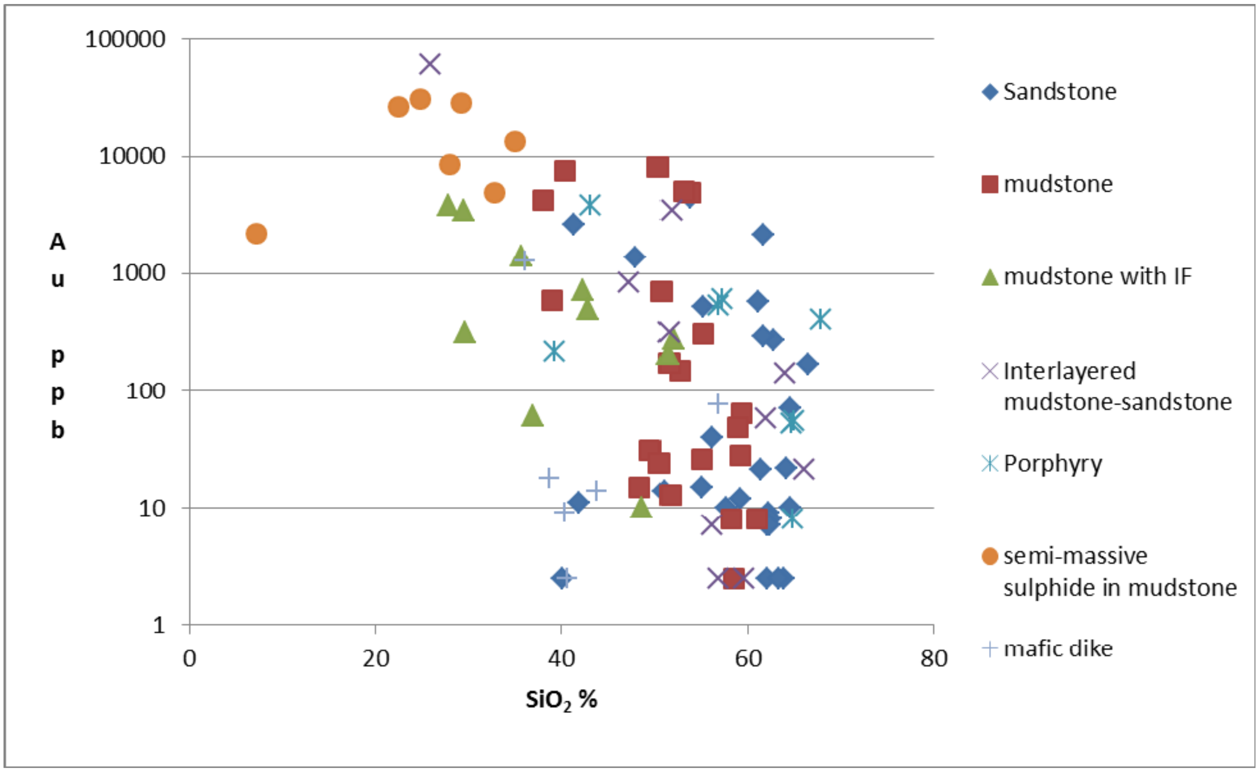

Figure 11: Au versus SiO_2 binary diagram

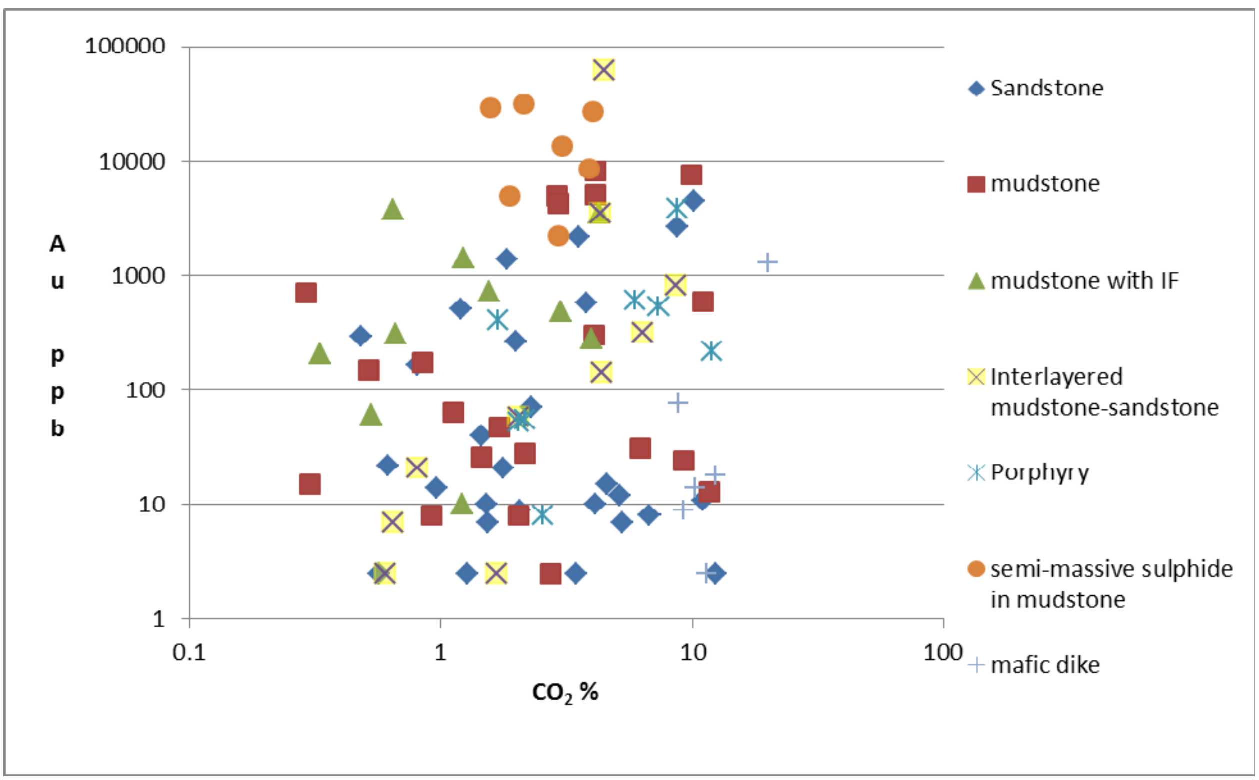

Figure 12: Au versus CO_2 binary diagram

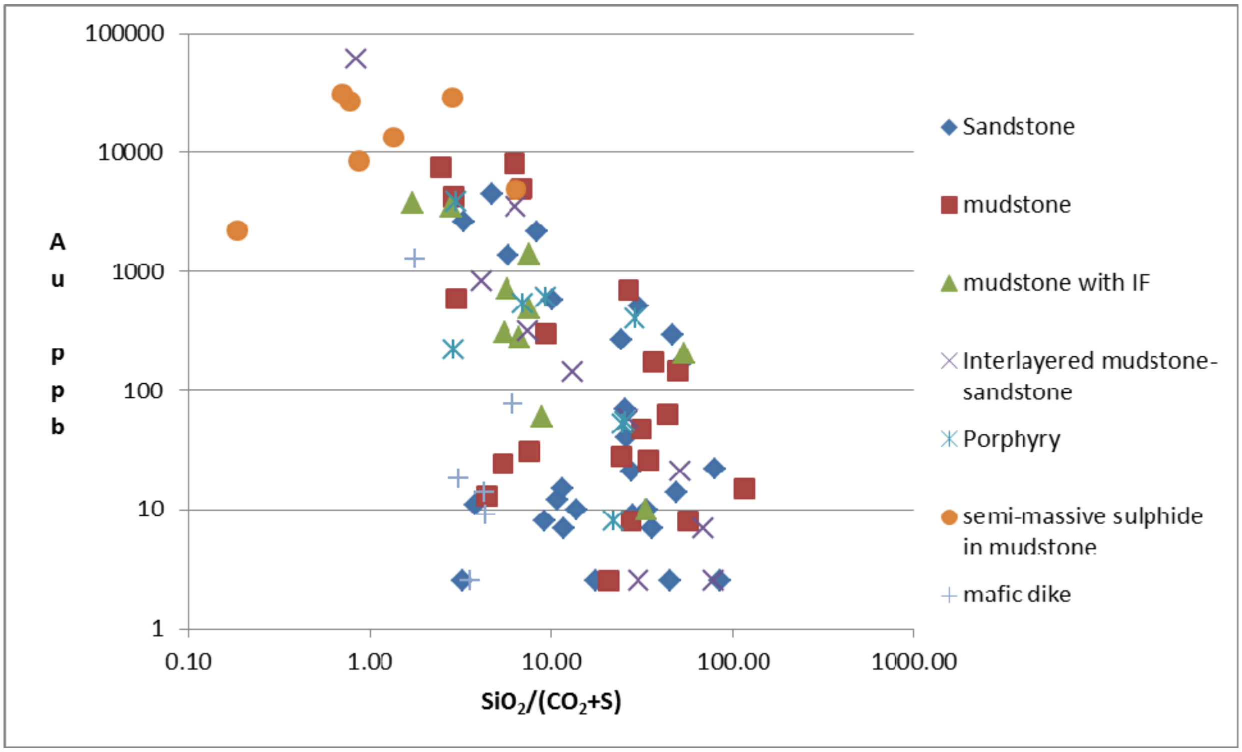

Figure 13: Au versus SiO_2 /(CO_2 + S) binary diagram

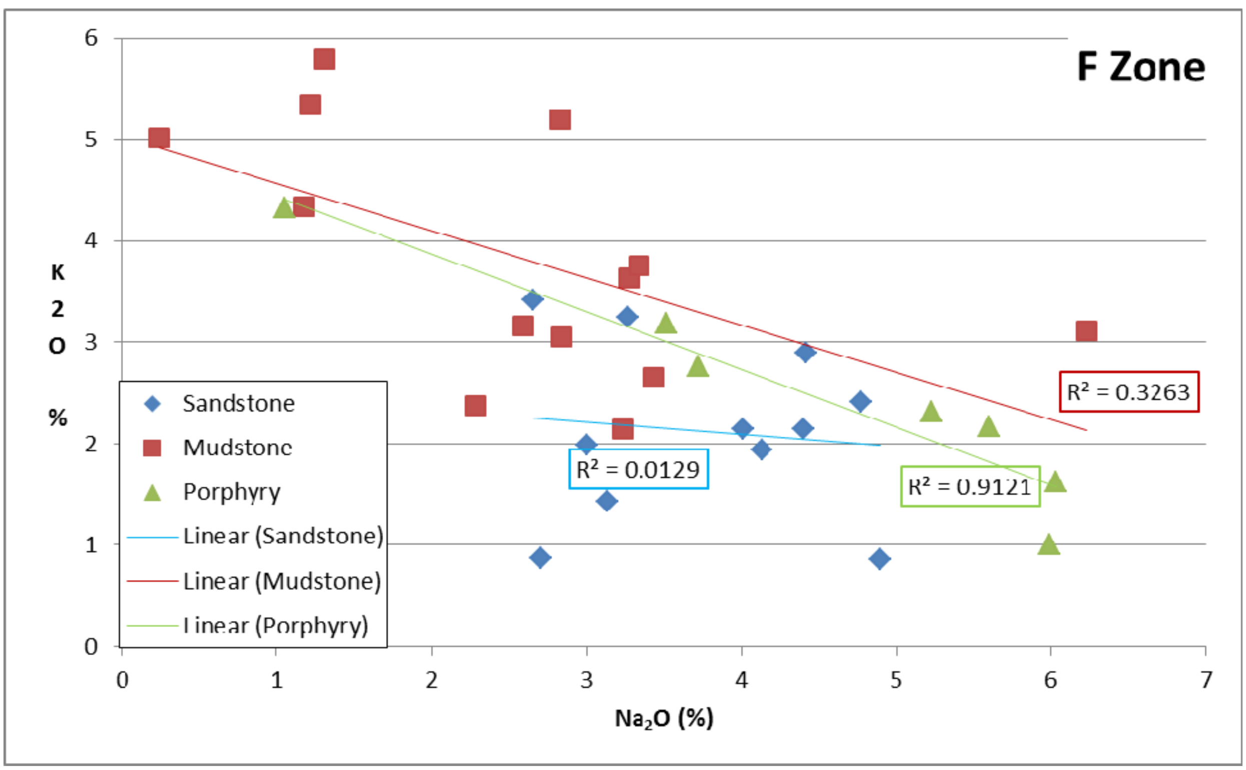

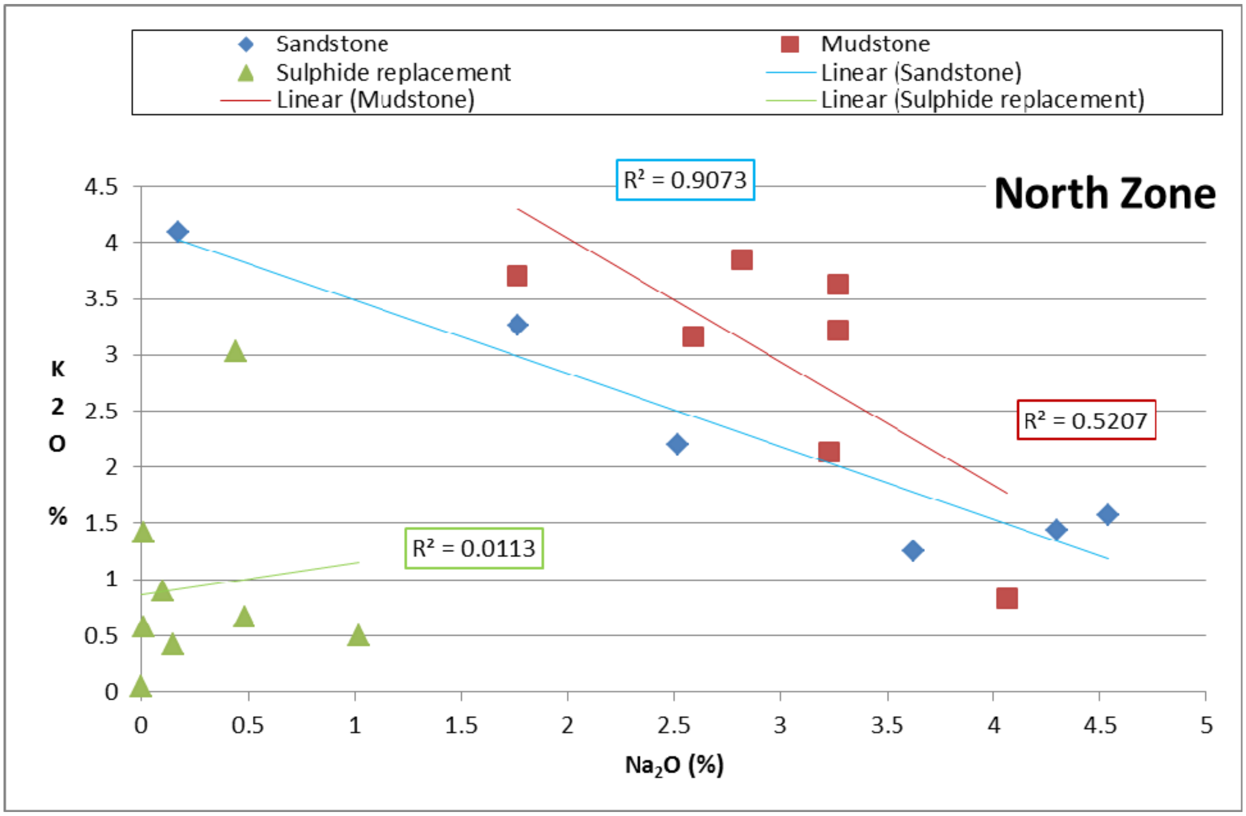

Figure 14: K_2O versus Na_2O binary diagrams

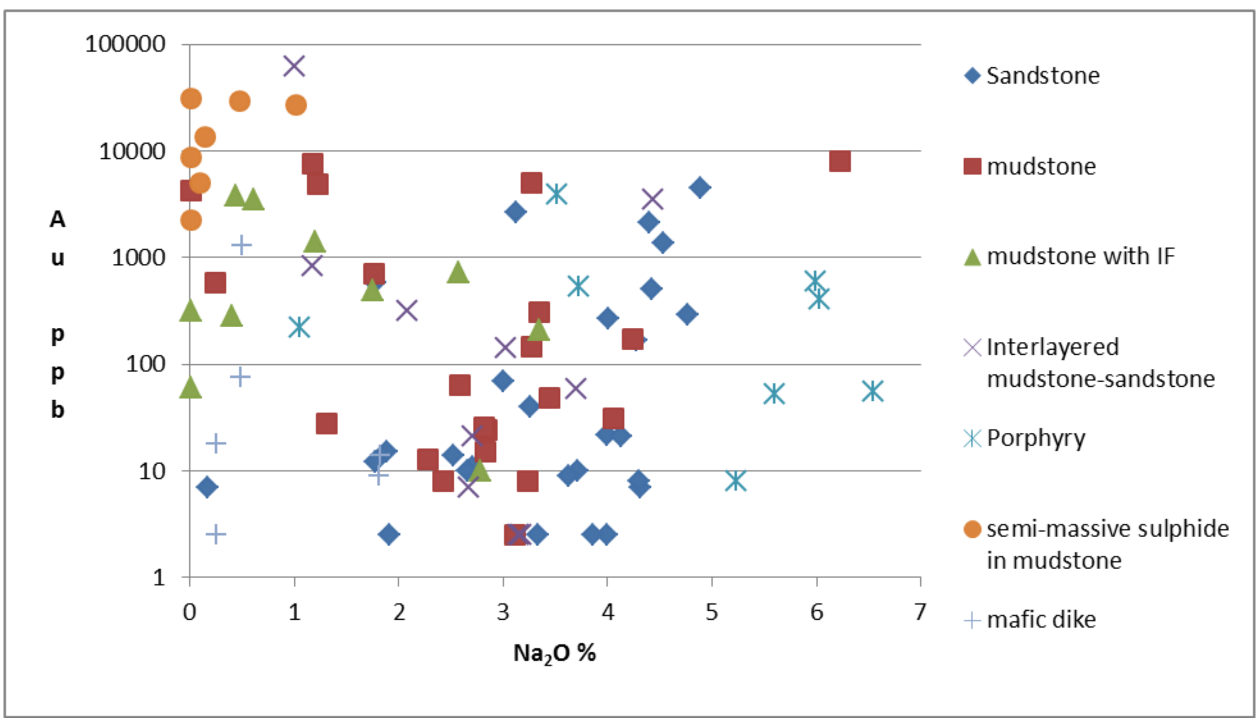

Figure 15: Au versus Na_2O binary diagram

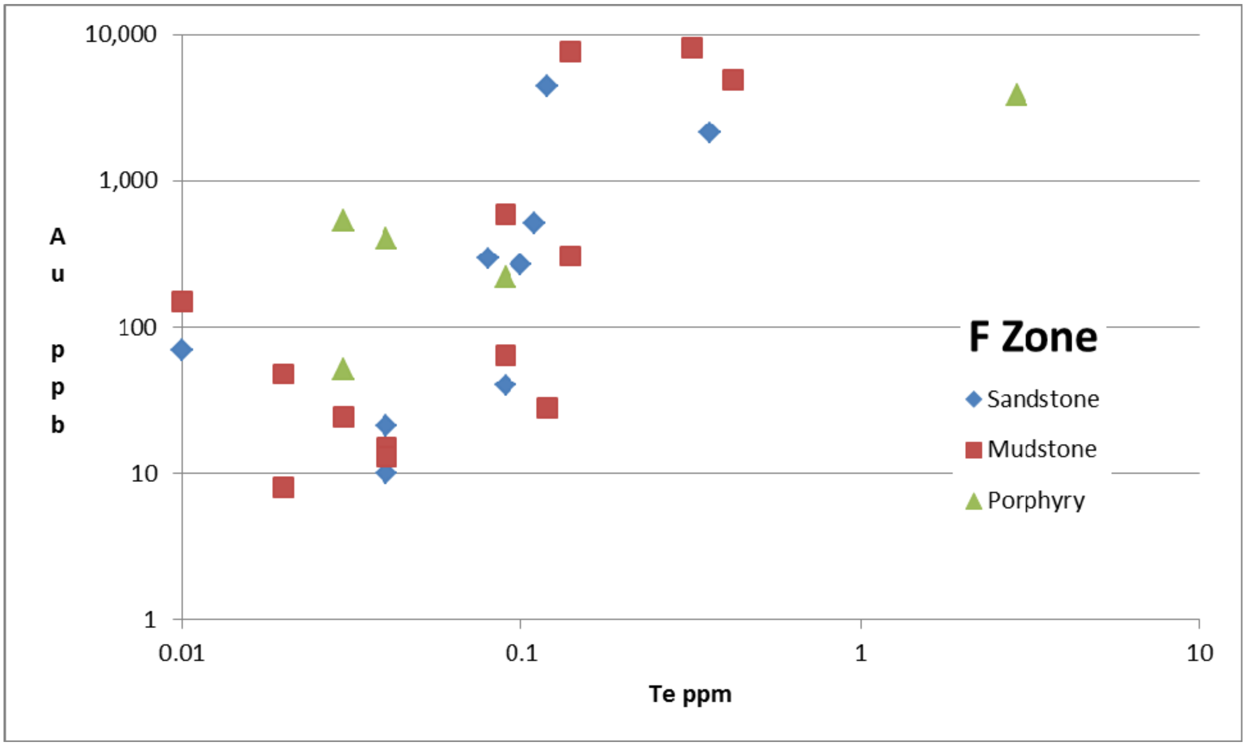

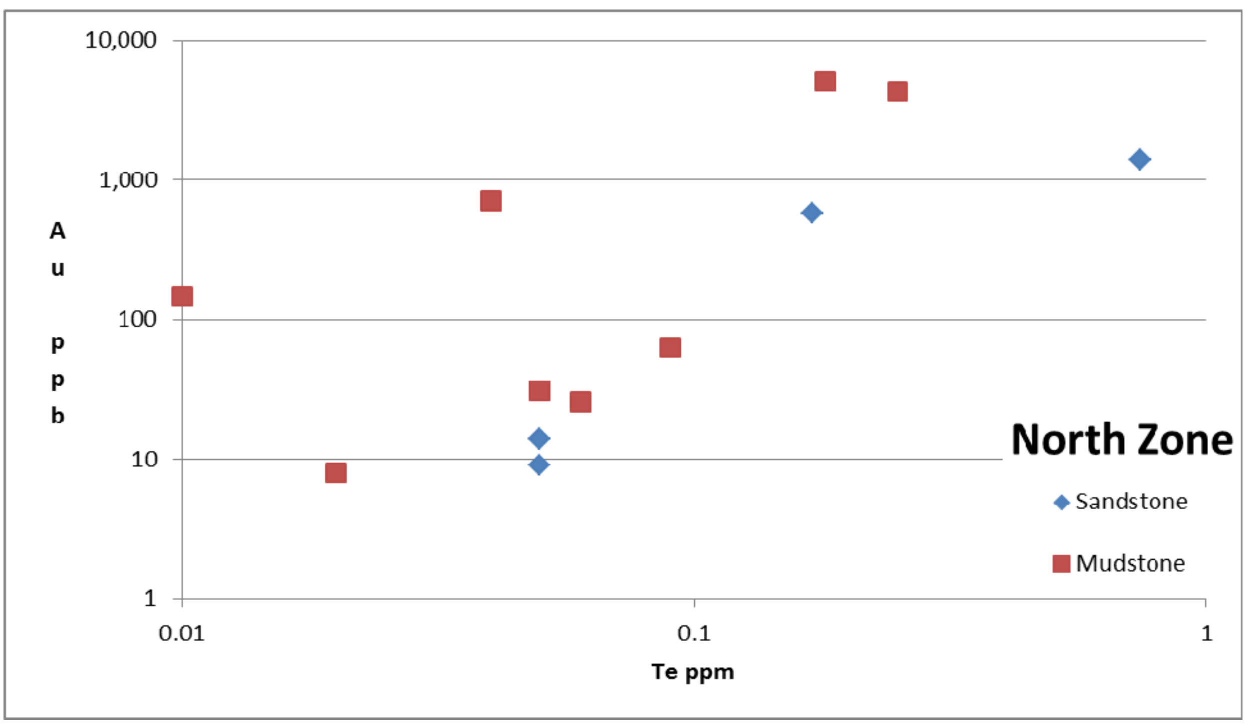

Figure 16: Au versus Te binary diagrams

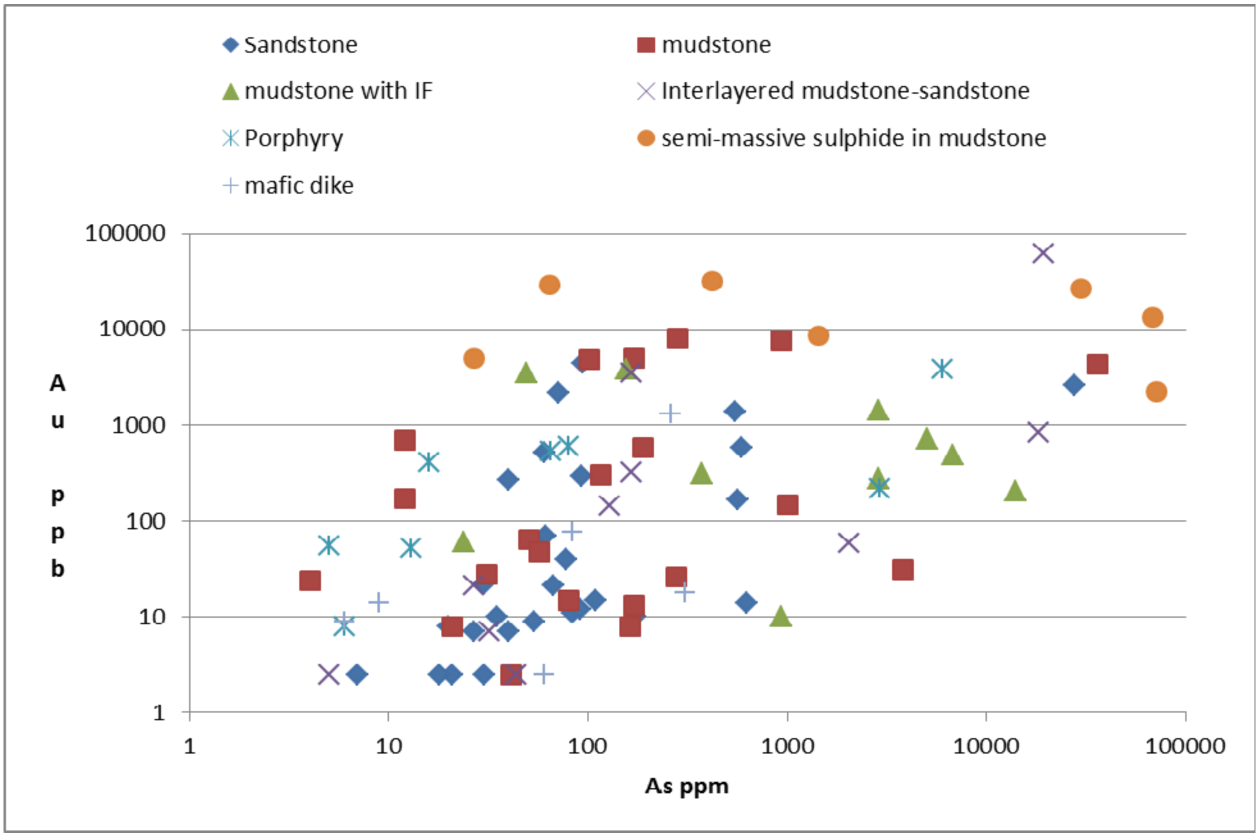

Figure 17: Au versus As binary diagram

Preliminary Conclusions

(1) The Geraldton area underwent three ductile deformation events (D_1 to D_3). Mineralization was emplaced syn-D_2 or early-D_3 as well as later during D_3. Thus, the mineralized zones in the Geraldton area formed during at least two mineralizing events.

(2) The F Zone is hosted by quartz-feldspar porphyry and interlayered sandstone and mudstones. It is characterized by quartz-ankerite±calcite veins with chlorite selvages and strong sericite-carbonate± chlorite alteration haloes. Sulphide minerals, such as pyrite +/- arsenopyrite +/- pyrrhotite +/- chalcopyrite, are present in the veins and their alteration haloes. The North Zone is characterized by gold-bearing semi-massive sulphide zones (pyrite +/- arsenopyrite +/- pyrrhotite +/- chalcopyrite) replacing beds in iron formation and possibly interlayered sandstone and mudstone. Folded quartz-ankerite±chlorite veins with chlorite and/or calcite selvages are associated with the semi-massive sulphide replacement zones.

(3) At the F Zone, magnetite, pyrrhotite and chalcopyrite in the altered wallrocks of quartz-ankerite veins were found as inclusions in coarser grained pyrite and arsenopyrite.

(4) At the North Zone, gold occurs as inclusions in pyrite and in fractures cutting through pyrite grains. As the main foliation (S_2?) in drill core commonly wraps around pyrite grains and euhedral arsenopyrite crystals occur along the foliation and later crenulations cleavage, this suggests that the emplacement and growth of sulphide minerals and possibly gold, span several deformation events or was emplaced in an active deformation zone with possible remobilization during a younger deformation.

(5) Preliminary geochemistry of altered rocks at the North Zone and F Zone suggests that i) gold grades are generally higher in rocks with higher total sulphur; ii) gold mineralization is associated with sulphidation and carbonation of the host rock, however, sulphidation seems to be the key process in gold enrichment; iii) the breakdown of feldspar during sericitization produced an inverse correlation between K_2O and Na_2O; iv) altered rocks with high Au values generally have high As and Te values.

References

Anglin, C.D. 1987. Geology, structure and geochemistry of gold mineralization in the Geraldton area, northwestern Ontario; Unpublished M.Sc. thesis, Memorial University of Newfoundland, St. John's, Newfoundland.

Anglin, C.D., Franklin, J.M., Loveridge, W.D., Hunt, P.A. and Osterberg, S.A. 1988. Use of zircon U-Pb ages of felsic intrusive and extrusive rocks in eastern Wabigoon Subprovince, Ontario, to place constraints on base metal and gold mineralization; *in* Radiogenic age and isotopic studies: report 2, Geological Survey of Canada, Paper 88-2, p.109-115.

Devaney, J.R. and Williams, H.R. 1989. Evolution of an Archean subprovince boundary: a sedimentological and structural study of part of the Wabigoon-Quetico boundary in northern Ontario; Canadian Journal of Earth Sciences, v.26, p.1013-1026.

Dubé B., Mercier-Langevin, P., Castonguay, S., McNicoll, V.J., Pehrsson, S.J., Bleeker, W., Schetselaar, E.M. and Jackson, S. 2011. Targeted Geoscience Initiative 4. Lode Gold Deposits in Ancient, Deformed and Metamorphosed Terranes—Footprints and Exploration Implications: A Preliminary Overview of Themes, Objectives andTargeted Areas; *in* Summary of Field Work and Other Activities 2011, Ontario Geological Survey, Open File Report 6270, p.38-1 to 38-10.

Eilu, P., Mikucki, E.J. and Dugdale, A.L. 2001. Alteration zoning and primary geochemical dispersion at the Bronzewing lode-gold deposit, Western Australia. Mineralium Deposita, v.36, p.13-31.

Hart, T.R., terMeer, M. and Jolette, C. 2002. Precambrian geology of Kitto, Eva, Summers, Dorothea, and Sandra Townships, northwestern Ontario: Phoenix bedrock mapping project; Ontario Geological Survey, Open File Report 6095, 206p.

Horwood, H.C. and Pye, E.G. 1955. Geology of Ashmore Township; Ontario Department of Mines, 60th Annual Report, v.60, Part 5, 105p.

Lafrance, B., DeWolfe, J.C. and Stott, G.M. 2004. A structural reappraisal of the Beardmore-Geraldton Belt at the southern boundary of the Wabigoon subprovince, Ontario, and implications for gold mineralization; Canadian Journal of Earth Sciences, v.41, p.217-235.

Lafrance, B., Tóth, Z., Dubé, B. and Mercier-Langevin, P. 2012. Targeted Geoscience Initiative 4. Lode Gold Deposits in Ancient Deformed and Metamorphosed Terranes: Geological Setting of Banded Iron Formation–Hosted Gold Mineralization in the Geraldton Area, Northern Ontario. Summary of Field Work and Other Activities 2012, Ontario Geological Survey, Open File Report 6280, p.48-1 to 48-10.

Macdonald, A.J. 1988. The Geraldton Gold Camp: The role of banded iron formation; Ontario Geological Survey, Open File Report 5694, 176p.

Mason, J. and White, G. 1986. Gold occurrences, prospects, and deposits of the Beardmore-Geraldton Area, districts of Thunder Bay and Cochrane; Ontario Geological Survey, Open File Report 5630, 680p.

Pye, E.G. 1952. Geology of Errington Township, Little Long Lac Area; Ontario Department of Mines, 60th Annual Report, v.60, Part 6, 140p.

Tomlinson, K.Y., Hall, R.P., Hughes, D.J. and Thurston, P.C. 1986. Geochemistry and assemblage accretion of metavolcanic rocks in the Beardmore-Geraldton greenstone belt, Superior Province; Canadian Journal of Earth Sciences, v.33, p.1520-1533.

Appendix:

Appendix includes:

- Location map for samples and drill holes (Figure 18-20.)
- Drill hole sections with location of samples (Figure 21- 22.)
- Detailed drill logs

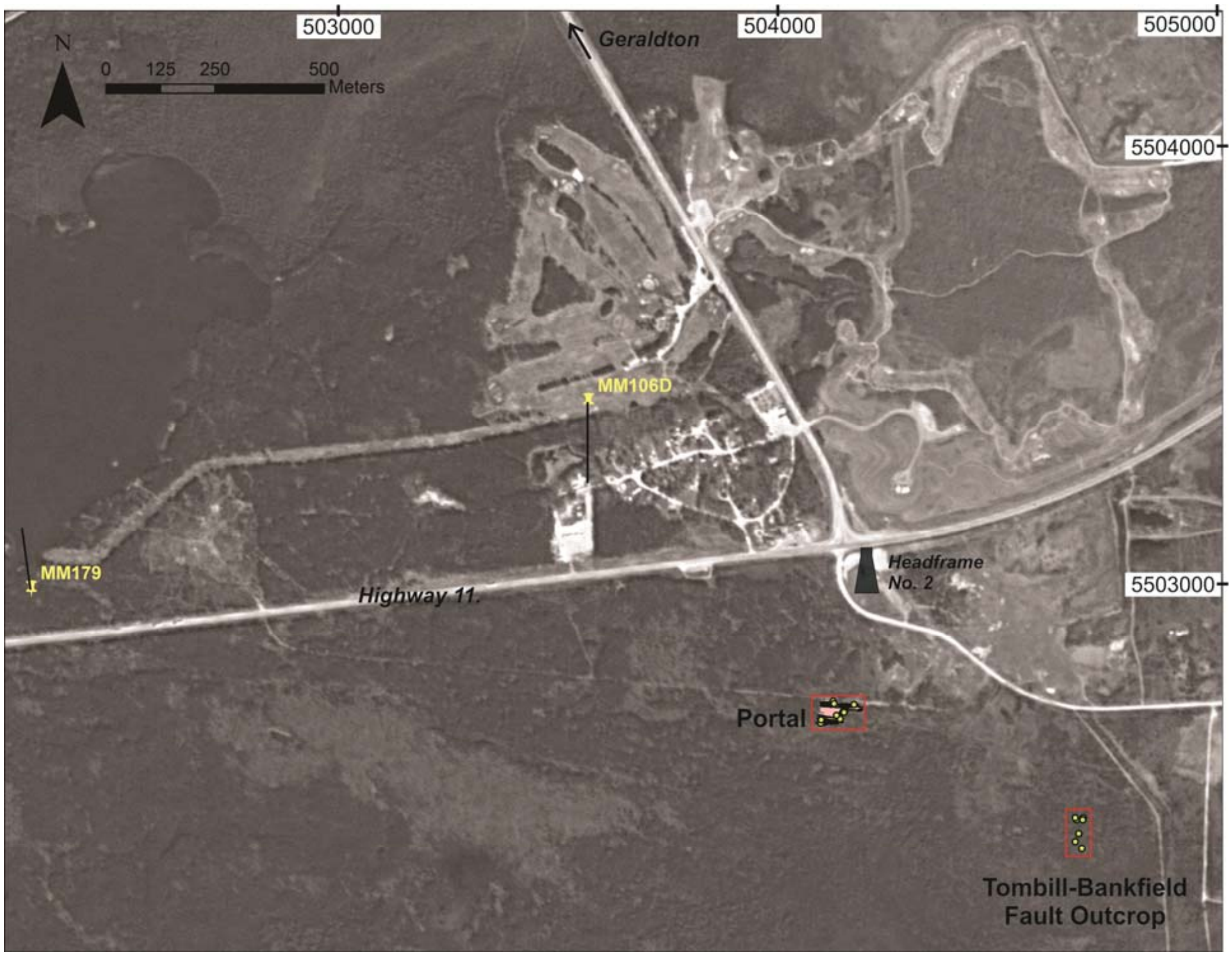

Figure 18: Location of the logged drill holes and mapped outcrops

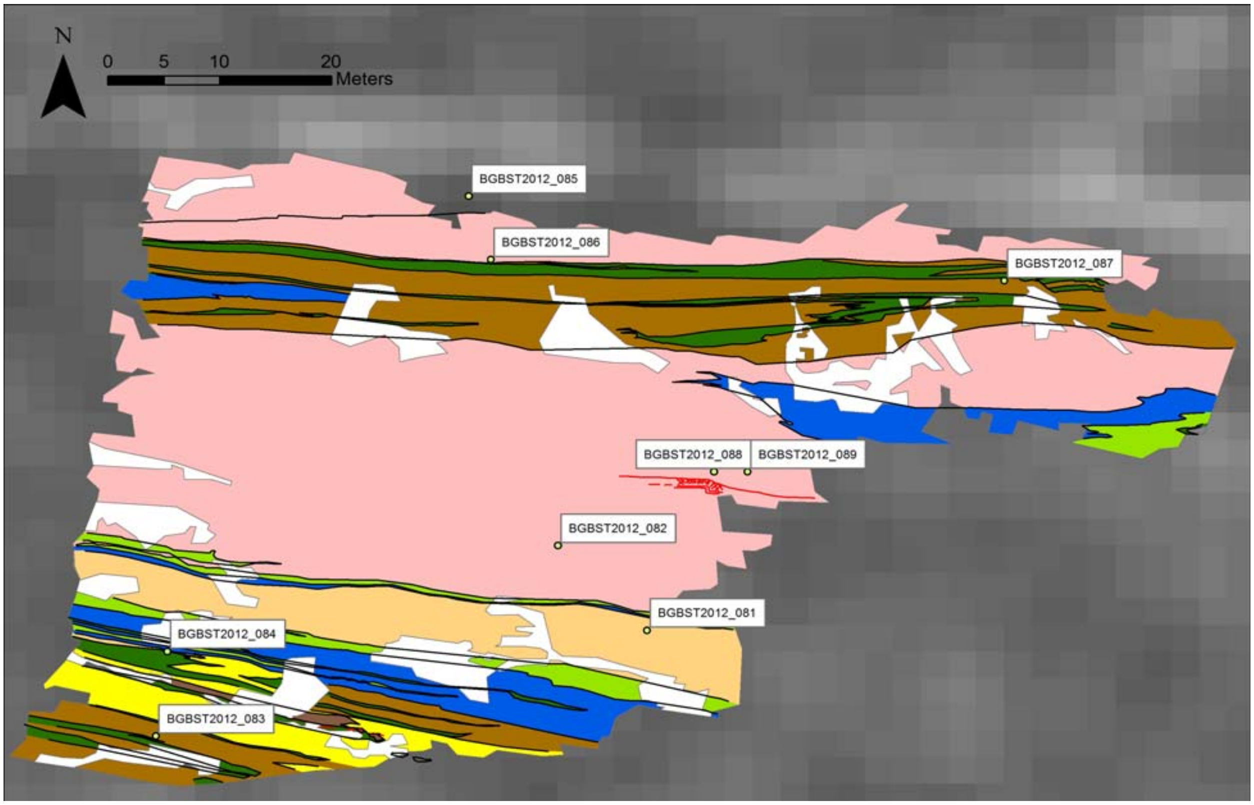

Figure 19: Location map for the samples on the Portal outcrop

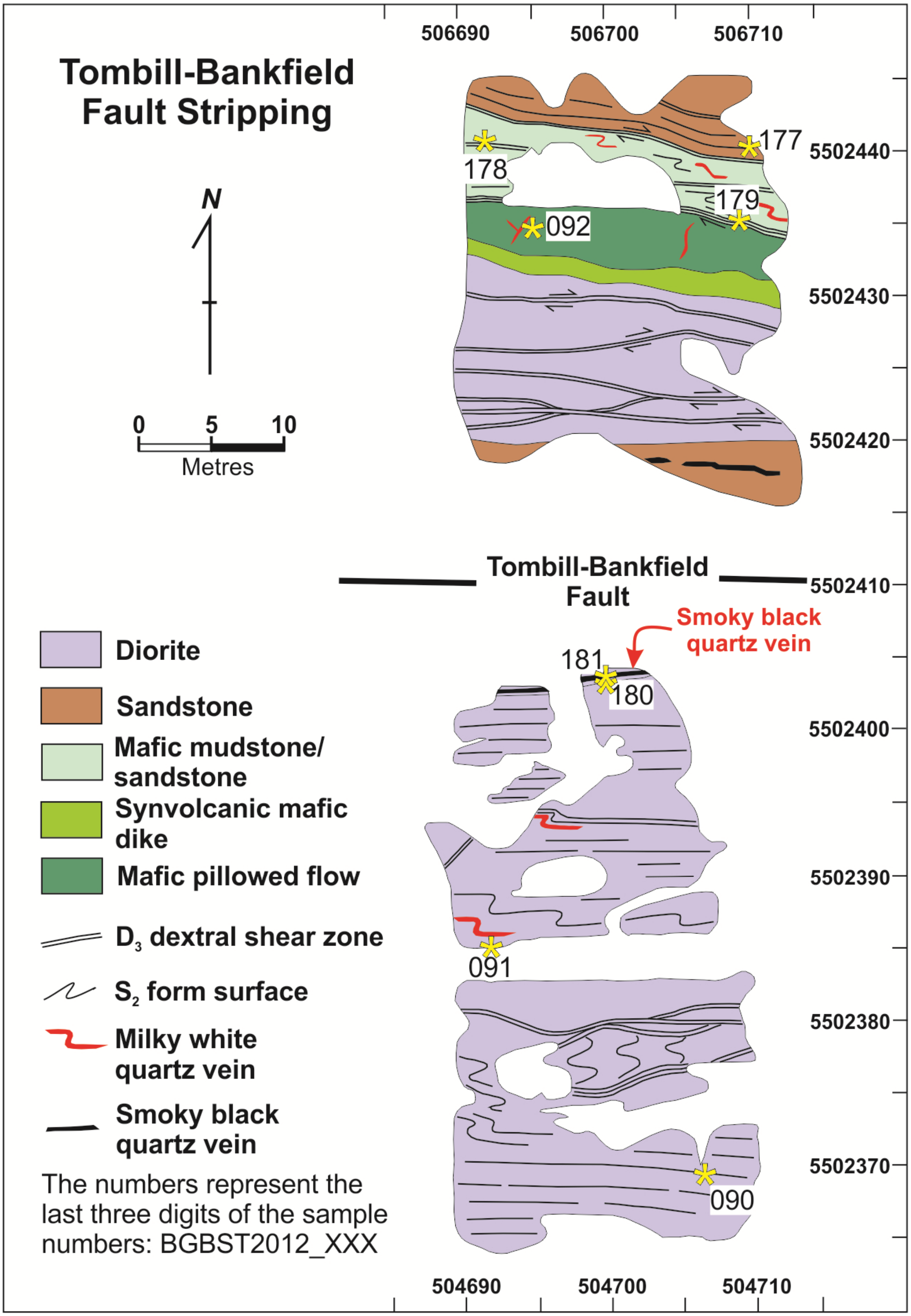

Figure 20: Location map for the samples on the Tombill-Bankfield Fault outcrop

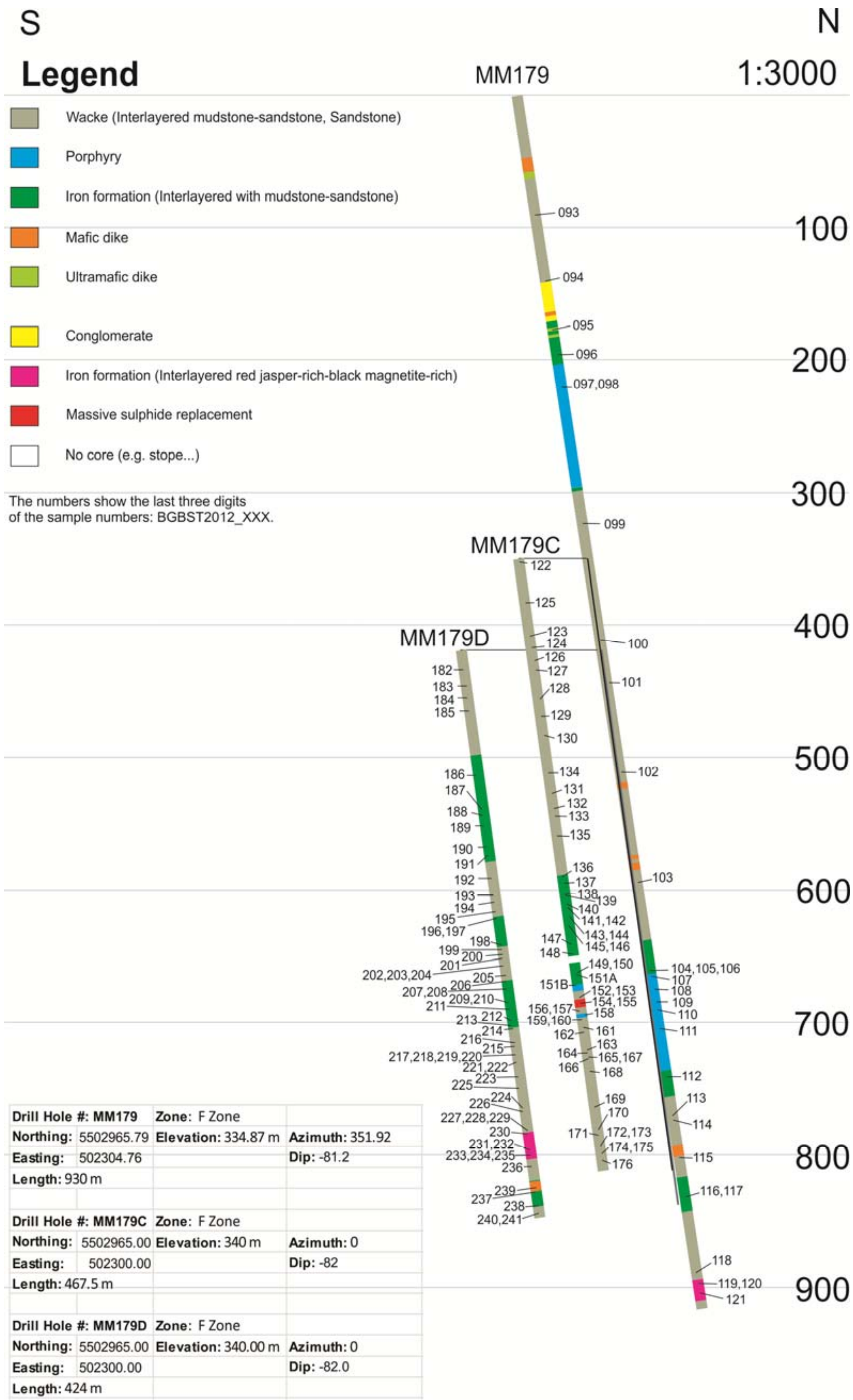

Figure 21. Section of MM 179, MM 179C and MM 179D drill holes.

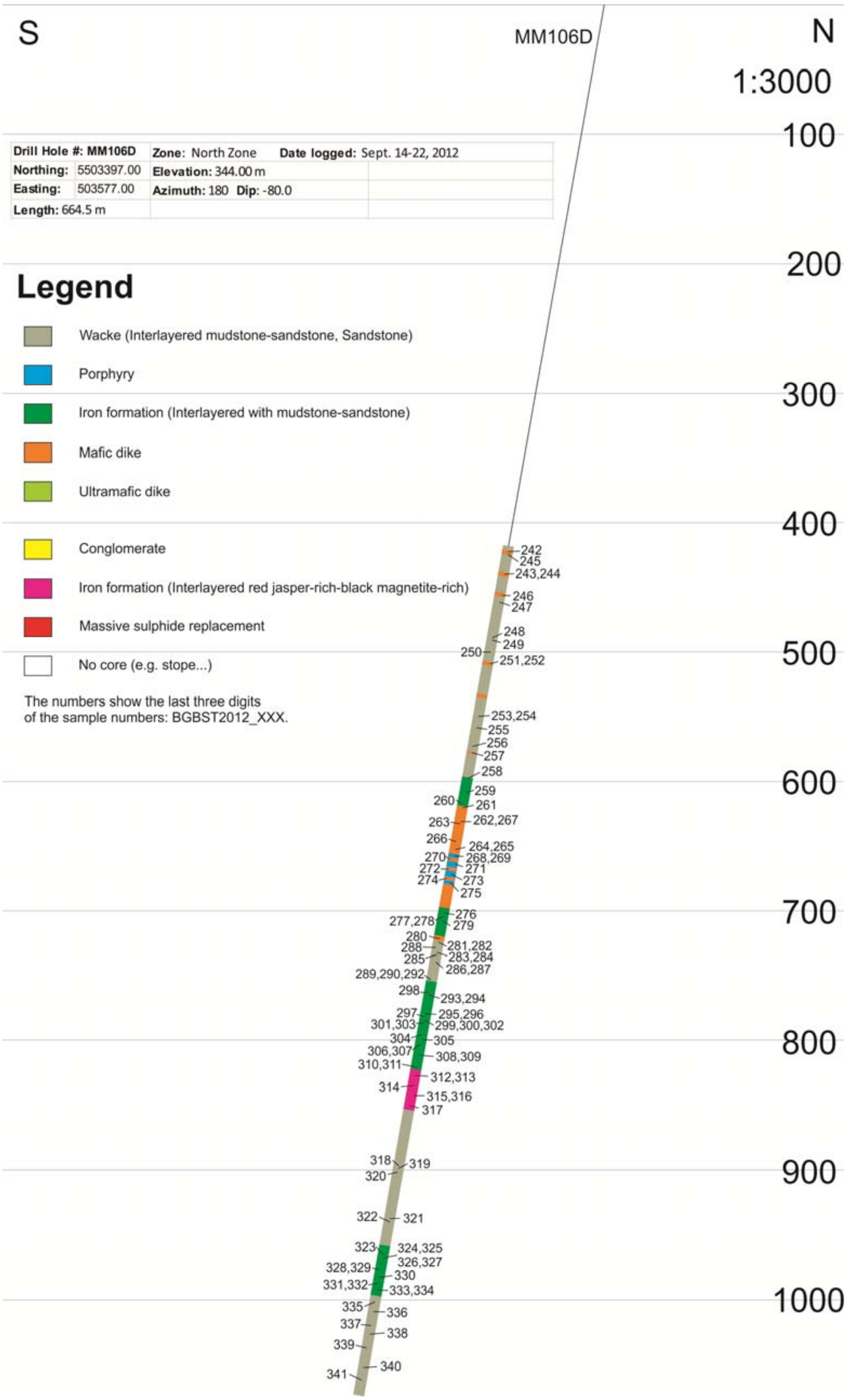

Figure 22. Section of MM 106 drill hole.

Sample #	Drill Hole #	Coordinates Northing	Easting	Interval (m) from	to	Lithology	Reason	Reason II.
BGBST2012_093	MM179	5502966	502305	87.00	87.35	Wacke		
BGBST2012_094	MM179	5502966	502305	136.82	137	Wacke	less altered	
BGBST2012_095	MM179	5502966	502305	172.83	172.95	Ultramafic dyke		
BGBST2012_096	MM179	5502966	502305	196.7	196.9	Sandstone	Calcitized average sandstone.	
BGBST2012_097	MM179	5502966	502305	218	218.18	Porphyry	highest analized value in the inteval	
BGBST2012_098	MM179	5502966	502305	218.87	219.05	Porphyry	pyrite-bearing alteration haloe around Q-turmaline vein	
BGBST2012_099	MM179	5502966	502305	320.65	321	Interlayered mudstone-sandstone	Average sample for this interval	
BGBST2012_100	MM179	5502966	502305	414.7	414.85	Interlayered mudstone-sandstone	Aspy containing sandstone with Q-ankerite veins	
BGBST2012_101	MM179	5502966	502305	440.3	440.5	Sandstone	Average sandstone, trace py	
BGBST2012_102	MM179	5502966	502305	511.65	511.93	Sandstone	Average sandstone with veins, py, apy	
BGBST2012_103	MM179	5502966	502305	591.25	591.55	Interlayered mudstone-sandstone	Average sandstone with veins and disseminated py (5%)	
BGBST2012_104	MM179	5502966	502305	657.13	657.33	Greenshale	Before SP zone with disseminated py-po and a vein of Q and minor ankerite	
BGBST2012_105	MM179	5502966	502305	657.78	657.98	Greenshale	SP zone: strongly chloritized, strongly folded rock with Q-Fe-crb. And py mostly po in microfractures	
BGBST2012_106	MM179	5502966	502305	658.9	659.1	Greenshale	SP zone: Strongly folded Q-crb. Veins, py-po fine veinlets parallel to the foliation with VG	
BGBST2012_107	MM179	5502966	502305	666.45	666.65	Porphyry	X zone: Characterized by disseminated py and also by Q-turmaline(?) vein	
BGBST2012_108	MM179	5502966	502305	675.14	675.34	Porphyry	Q-chlorite vein with silicification around the margin of the vein. Disseminated py. Representative of the pervasive very low grade mineralization through the porphyry.	
BGBST2012_109	MM179	5502966	502305	685.37	685.64	Porphyry	Wide Q-chlorite vein cut across Q-fsp. Veins. Disseminated py.	
BGBST2012_110	MM179	5502966	502305	692.25	692.45	Porphyry	Higher gold value associated with a few narrow veins (< 1cm). Dissmeninated py-po-apy.	
BGBST2012_111	MM179	5502966	502305	707	707.38	Porphyry	Coarse and fine grained porphyry in the same sample without sharp contact.	
BGBST2012_112	MM179	5502966	502305	744.13	744.33	Interlayered mudstone-sandstone	Strongly deformed mineralization with yellowish alteration with strong py-po-apy dissemination	
BGBST2012_113	MM179	5502966	502305	767.4	767.7	Interlayered mudstone-sandstone	Apy needles around Q-crb. Vein	
BGBST2012_114	MM179	5502966	502305	774.35	774.45	Interlayered mudstone-sandstone	Q veins with strong Fe-crb. Alteration and disseminated py-po in alteration haloe	F Zone
BGBST2012_115	MM179	5502966	502305	804.44	804.62	Interlayered mudstone-sandstone	A 4 mm speck of gold in a Q-vein associated with a very weak alteration haloe. Very weak dissem. Py around alt. haloe	
BGBST2012_116	MM179	5502966	502305	835.95	836.13	Iron formation with greenshale.	Q-veins with py replacing IF. Vein is parallel to the axial plane of folds.	
BGBST2012_117	MM179	5502966	502305	837.43	837.69	Iron formation with greenshale.	Possibly refolded fold in IF	
BGBST2012_118	MM179	5502966	502305	883.7	883.95	Sandstone	Q-ankerite veins with po-py-apy and alteration haloe.	
BGBST2012_119	MM179	5502966	502305	898.9	898.67	Iron formation	Massive po-py above the dike(?).	
BGBST2012_120	MM179	5502966	502305	898.9	899.24	Iron formation	Dyke with strong chlorite-Fe-crb. Alteration and veins along it with 5-10 % py-apy	
BGBST2012_121	MM179	5502966	502305	903.65	904.05	Iron formation	Best mineralized interval in IF, but no sulphides. It shows the 2 generations of folds.	
BGBST2012_122	MM179C	5502965	502300	355.6	355.85	Interlayered mudstone-sandstone	The second generation of veins is cut by the third py-bearing veins	

Sample #	Drill Hole #	Coordinates Northing	Easting	Interval (m) from	to	Lithology	Reason	Reason II.
BGBST2012_123	MM179C	5502965	502300	409.35	409.58	Interlayered mudstone-sandstone	Q-ankerite veins are cutting across early calcite veins.	
BGBST2012_124	MM179C	5502965	502300	418.3	418.45	Interlayered mudstone-sandstone	Late calcite vein is cutting through the early calcite vein/bands.	
BGBST2012_125	MM179C	5502965	502300	384.15	384.36	Sandstone	Protolit sandstone	
BGBST2012_126	MM179C	5502965	502300	424.53	424.66	Interlayered mudstone-sandstone	Veins/Fractures are filled by py-po-cpy-apy?	
BGBST2012_127	MM179C	5502965	502300	432.34	432.49	Interlayered mudstone-sandstone	Calcite-Q vein overprinted Fe-crb. Vein	
BGBST2012_128	MM179C	5502965	502300	449.55	449.76	Interlayered mudstone-sandstone	Q-ankerite vein cutting through the ankerite band.	
BGBST2012_129	MM179C	5502965	502300	460.6	460.7	Lamprophyre	Lamprophyre dike	
BGBST2012_130	MM179C	5502965	502300	479.05	479.35	Interlayered mudstone-sandstone	Py-po-apy associated with Q-ankerite vein with moderate chloritic selvage	
BGBST2012_131	MM179C	5502965	502300	525.6	525.85	Interlayered mudstone-sandstone	Crosscutting relationship between early Fe-band and a younger Q-vein	
BGBST2012_132	MM179C	5502965	502300	543.4	543.87	Interlayered mudstone-sandstone	Strong Fe-carbonatic alteration without a sharp contact to its host rock. This assamblage was often described as a strongly altered dike, but I do not agree. At the contact, it contains calcite veins.	
BGBST2012_133	MM179C	5502965	502300	548.8	549	Interlayered mudstone-sandstone	Quartz-ankerite/feldspar vein for study of vein-filling.	
BGBST2012_134	MM179C	5502965	502300	514.9	515	Sandstone	Control sample for weakly calcitized sandstone	
BGBST2012_135	MM179C	5502965	502300	567.15	567.24	Sandstone	Control sample for moderately calcitized sandstone	
BGBST2012_136	MM179C	5502965	502300	588.13	588.64	Interlayered mudstone-sandstone-IF	Control sample from interlayered mudstone-sandstone with IF bands	
BGBST2012_137	MM179C	5502965	502300	595.8	596	Interlayered mudstone-sandstone	Biotite-chlorite-pyrite occurs in veins and alteration haloe, strongly def. (boudinaged+folded) veins out of the mineralization, disseminated py	
BGBST2012_138	MM179C	5502965	502300	603.58	603.81	Interlayered mudstone-sandstone-IF	Quartz-ankerite veins with pyrite-bearing haloe	Determine the alteration style for veins in sandstone
BGBST2012_139	MM179C	5502965	502300	605.5	605.7	mudstone	Quartz-ankerite veins with sericitic haloe, fine grained disseminated sulphide	
BGBST2012_140	MM179C	5502965	502300	611.5	611.74	Sandstone	Carbonatic alteration haloe around quartz-carbonate(calcite+ankerite) with disseminated py and apy in the alteration haloe in sandstone	
BGBST2012_141	MM179C	5502965	502300	616.73	617.03	mudstone	SP Zone: Carbonatic alteration haloe with disseminated py in sandstone and probably sericitic alteration haloe in mudstone	Shows the youngest clevage.
BGBST2012_142	MM179C	5502965	502300	617.24	617.39	Interlayered mudstone-sandstone-IF	Sericitic alteration haloe overprinted by a young, Q-calcite vein. Q-ankerite veins and their haloe overprint Fe-carbonate bands, these are overprinted by a narrow, mm-wide Q-calcite vein.	Vein generations.
BGBST2012_143	MM179C	5502965	502300	620.3	620.62	Interlayered mudstone-sandstone-IF	Quartz-crb. Vein containing po altered fragment and surrounded by a haloe of 10 % po. A half meter before IF.	
BGBST2012_144	MM179C	5502965	502300	621	621.19	Interlayered mudstone-sandstone-IF	IF bands replaced by mostly po and monor apy. Calcite veins occur probably parallel to the axial plane of folds.	

Sample #	Drill Hole #	Coordinates Northing	Easting	Interval (m) from	to	Lithology	Reason	Reason II.
BGBST2012_145	MM179C	5502965	502300	631.46	631.67	Interlayered mudstone-sandstone-IF	Q-ank. Vein with bleached po-bearing alt. haloe.	
BGBST2012_146	MM179C	5502965	502300	632.55	633	Interlayered mudstone-sandstone-IF	Po-rich band in IF which is cut by py-po-chl. Veins.	
BGBST2012_147	MM179C	5502965	502300	643.6	643.8	Interlayered mudstone-sandstone-IF	Ankerite vein with chlorite haloe overprinting ankerite bands	
BGBST2012_148	MM179C	5502965	502300	648.9	649.1	mudstone	Quartz-ankerite veins with chlorite-bitotite selvage, py, apy, po.	
BGBST2012_149	MM179C	5502965	502300	664.9	665.16	Interlayered mudstone-sandstone-IF	Boudinaged IF bands Q-veins in neck of boudinsand replacement of coarse grained apy.	
BGBST2012_150	MM179C	5502965	502300	665.68	665.82	Interlayered mudstone-sandstone-IF	IF bands replaced by po with late py-chl. Cut by Q-ank. Francture in the fold hinge in Q-ank. Vein filled with po.	
BGBST2012_151A	MM179C	5502965	502300	666.07	666.27	Interlayered mudstone-sandstone-IF	Disseminated po replacing IF, itself is replaced by coarse apy. Q veins and py are emplaced in fractures due to boudinage prior to folding of IF bands.	
BGBST2012_151B	MM179C	5502965	502300	670.2	670.33	Porphyry	F Zone: Vein with alteration haloe	
BGBST2012_152	MM179C	5502965	502300	677.5	677.9	Interlayered mudstone-sandstone	F Zone: Strong sericitic alteration haloe with vein of Q-ank-gold. Apy-py in alteration haloe.	
BGBST2012_153	MM179C	5502965	502300	679.38	679.56	Interlayered mudstone-sandstone	F Zone: Boudinaged and folded Q vein with strong sericitic alteration haloe with py only.	
BGBST2012_154	MM179C	5502965	502300	681.27	681.5	Semi-massive sulphide	F Zone: Semi-massive py-apy bands around a Q-ankerite -gold vein and sericitic alt. haloe	
BGBST2012_155	MM179C	5502965	502300	685.05	685.25	Semi-massive sulphide	F Zone: Apy-rich banded semi-massive sulphide and sericite alt. haloe	
BGBST2012_156	MM179C	5502965	502300	688.29	688.44	Interlayered mudstone-sandstone	F Zone: Uniformly altered (sericite) rock that contains sulphides (pyrite) along foliation.	
BGBST2012_157	MM179C	5502965	502300	688.55	688.77	Interlayered mudstone-sandstone	F Zone: Quartz-ankerite veins with gold	
BGBST2012_158	MM179C	5502965	502300	689.65	690	Porphyry	F Zone: Silicified porphyry with 5% py	
BGBST2012_159	MM179C	5502965	502300	693.44	693.55	Interlayered mudstone-sandstone	F Zone: Py and po in late francture in a Q-ank. Vein	
BGBST2012_160	MM179C	5502965	502300	697.8	697.9	Interlayered mudstone-sandstone	F Zone: Banded apy-po overprinted by py in black mudstone.	
BGBST2012_161	MM179C	5502965	502300	704.27	704.57	Interlayered mudstone-sandstone	Two strongly def. Q-ank veins with sericitic alt. haloe with py.	
BGBST2012_162	MM179C	5502965	502300	708.3	708.6	Interlayered mudstone-sandstone	Strongly deformed Q-ankerite vein with disseminated py in sericitic alteration haloe. Last observed alteration haloe around Q-ank. Veins.	
BGBST2012_163	MM179C	5502965	502300	720	720.38	Interlayered mudstone-sandstone-IF	F Zone: Strong sericitic alteration with py-apy associated with gold-bearing Q-ankerite veins.	
BGBST2012_164	MM179C	5502965	502300	724.6	725	Interlayered mudstone-sandstone-IF	F Zone: Po bands overprinted by coarse grained py with chlorite selvage.	
BGBST2012_165	MM179C	5502965	502300	729.45	729.65		Chlorite veins associated with po seems to appear in the neck of the boudins of Q-ank veins	noname mineralization
BGBST2012_166	MM179C	5502965	502300	732.74	732.94	Interlayered mudstone-sandstone	Crosscutting relationship between Q-calcite vein and another mostly Q vein. Minor py-apy bith in veins and in sandstone.	
BGBST2012_167	MM179C	5502965	502300	730.49	730.8	Interlayered mudstone-sandstone	Alteration haloe around Q-ankerite vein with disseminated py	

Sample #	Drill Hole #	Coordinates Northing	Easting	Interval (m) from	to	Lithology	Reason	Reason II.
BGBST2012_168	MM179C	5502965	502300	740.82	741	Interlayered mudstone-sandstone	Biotite around Q-ank vein	
BGBST2012_169	MM179C	5502965	502300	763.53	763.7	Interlayered mudstone-sandstone	Biotite in chloritic selvage around Q-ankerite vein	
BGBST2012_170	MM179C	5502965	502300	789.95	790.21	Interlayered mudstone-sandstone	Fortune zone: Average sample with veins of Q-ankerite-calcite with py-po stringers	
BGBST2012_171	MM179C	5502965	502300	792.12	792.27	Interlayered mudstone-sandstone	Po in calcite vein without gold.	
BGBST2012_172	MM179C	5502965	502300	795.6	795.83	Interlayered mudstone-sandstone	Collected to examine the relationship of the veins.	
BGBST2012_173	MM179C	5502965	502300	794.62	794.7	Interlayered mudstone-sandstone	Control sample for the strongly chloritized-carbonatized zone.	
BGBST2012_174	MM179C	5502965	502300	798.7	798.95	Interlayered mudstone-sandstone	Py-po with strongly deformed Q-ankerite vein	
BGBST2012_175	MM179C	5502965	502300	799.17	799.58	Interlayered mudstone-sandstone	Collected to examine the relationship of the veins.	
BGBST2012_176	MM179C	5502965	502300	803.03	803.2	Sandstone	Sandstone without gold	
BGBST2012_182	MM179D	5502965	502300	433.6	433.94	Sandstone	Chlorite-calcite vein cut across quartz-ankerite/feldspar? Vein in sandstone. Pyrite-pyrrhotite associated with calcite veins and chlorite selvage.	
BGBST2012_183	MM179D	5502965	502300	456	456.15	Interlayered mudstone-sandstone	Ankerite vein cut across quartz-ankerite/feldspar? It also contains younger calcite-chlorite vein with pyrite and pyrrhotite.	
BGBST2012_184	MM179D	5502965	502300	463.19	463.32	Mafic dike	Mafic dike.	
BGBST2012_185	MM179D	5502965	502300	472.06	472.23	Sandstone	Sandstone protolit. Moderately calcitized. Disseminated py	
BGBST2012_186	MM179D	5502965	502300	517.6	517.79	Interlayered mudstone-sandstone	Biotite appears around around both quartz and calcite vein associated with chlorite, pyrite and pyrrhotite.	
BGBST2012_187	MM179D	5502965	502300	543	543.21	Iron formation with greenshale.	Iron formation containing greenshale (green mudstone) with semi-massive pyrite-calcite and pyrrhotite-calcite veins replacing thin magnetite-bearing layers.	
BGBST2012_188	MM179D	5502965	502300	549.21	549.47	Interlayered mudstone-sandstone	Highest analized gold value in the inteval. Greenish grey sandstone-mudstone with quartz-calcite veins associated with pyrite-pyrrhotite and disseminated pyrite.	
BGBST2012_189	MM179D	5502965	502300	555.41	555.59	Interlayered mudstone-sandstone	Yellowish alteration haloe around quartz-calcite veins with fine grained disseminated sulphide (pyrite).	
BGBST2012_190	MM179D	5502965	502300	569.65	569.81	Sandstone	Calcitized average sandstone with disseminated sulphide.	
BGBST2012_191	MM179D	5502965	502300	576	576.2	Iron formation with greenshale.	Greenshale with iron formation with calcite-pyrite veins within iron formation and disseminated pyrite.	
BGBST2012_192	MM179D	5502965	502300	592.5	592.75	Sandstone	Very strong calcitization and chloritization most probably in sandstone but the original lithology can not be determined, because of the strong alteration.	
BGBST2012_193	MM179D	5502965	502300	603.8	604.17	Sandstone	This represents the entire interval. Quartz-calcite vein with chloritic selvage and sulphides in it (pyrite-pyrrhotite). Weak disseminated arsenopyrite also appears in the sandstone.	
BGBST2012_194	MM179D	5502965	502300	605	605.18	Interlayered mudstone-sandstone	Quartz-calcite veins with sulphides and chlorite-sericite selvage.	

Sample #	Drill Hole #	Coordinates Northing	Easting	Interval (m) from	to	Lithology	Reason	Reason II.
BGBST2012_195	MM179D	5502965	502300	612.27	612.68	Interlayered mudstone-sandstone	Strong sericitic haloe appears with 10 % disseminated pyrite and minor pyrrhotite at the end of this interval.	
BGBST2012_196	MM179D	5502965	502300	613.61	614.15	Iron formation with greenshale.	Semi-massive sulphide replacement in iron formation in green mudstone (greenshale).	
BGBST2012_197	MM179D	5502965	502300	614.57	614.67	Iron formation with greenshale.	Weak arsenopyrite-pyrite replacement in iron formation.	
BGBST2012_198	MM179D	5502965	502300	635.05	635.28	Iron formation with greenshale.	Iron formation bands replaced with 5 % arsenopyrite associated with quartz-calcite veins in green mudstone (greenshale).	
BGBST2012_199	MM179D	5502965	502300	639.38	639.58	Sandstone	Average sandstone.	
BGBST2012_200	MM179D	5502965	502300	643	643.55	Interlayered mudstone-sandstone	Strong 3-4 % pyrite-bearing, yellowish (sericitic) alteration haloe around quartz-calcite-pyrrhotite veins.	
BGBST2012_201	MM179D	5502965	502300	649.25	649.67	Interlayered mudstone-sandstone	Pyrite and pyrrhotite-bearing quartz-ankerite-calcite veins and weak pyrite-bearing, probably sericitic alteration haloe. Quartz-ankerite/feldspar? Veins cut across these veins.	
BGBST2012_202	MM179D	5502965	502300	654.3	654.57	Interlayered mudstone-sandstone	Quartz-ankerite/feldspar? Veins with strong sericite-ankerite alteration haloe with disseminated pyrite.	
BGBST2012_203	MM179D	5502965	502300	656	656.48	Interlayered mudstone-sandstone	Quartz-ankerite veins with sericite-ankerite alteration haloe with disseminated pyrite and quartz-ankerite-calcite-pyrrhotite veins with chlorite selvage. Disseminated arsenopyrite appears between these veins.	
BGBST2012_204	MM179D	5502965	502300	658.61	658.86	Interlayered mudstone-sandstone	Pyrite-bearing sericite alteration haloe overprinting chlorite around quartz-ankerite/feldspar? Vein that also contains pyrite-chalcopyrite-pyrrhotite.	
BGBST2012_205	MM179D	5502965	502300	665.44	665.71	Sandstone	Average alightly ankeritized and chloritized sandstone.	
BGBST2012_206	MM179D	5502965	502300	669.24	669.49	Interlayered mudstone-sandstone-IF	Pyrite and pyrrhotite replace iron formation around quartz-ankerite? Vein	
BGBST2012_207	MM179D	5502965	502300	674.45	674.58	Interlayered mudstone-sandstone-IF	Green vein cutting through iron formation. Arsenopyrite emplaced in iron formation and in the vein.	
BGBST2012_208	MM179D	5502965	502300	676.1	676.2	Interlayered mudstone-sandstone-IF	Pyrite veinlets cutting through the iron formation.	
BGBST2012_209	MM179D	5502965	502300	685	685.38	Interlayered mudstone-sandstone-IF	Quartz-ankerite vein with pyrite-bearing sericite alteration haloe and another quartz-ankerite? Vein with narrow chlorite selvage that contains arsenopyrite and pyrrhotite.	
BGBST2012_210	MM179D	5502965	502300	688.88	689.12	mudstone	Sericitic alteration haloe in mudstone. Sulphide (pyrite) appears mostly in vein. Quartz-ankerite? Vein cut through ankerite-quartz vein.	
BGBST2012_211	MM179D	5502965	502300	694.72	694.92	Interlayered mudstone-sandstone-IF	Boudinaged ankerite? Veins. Quarts is emplaced in extensional veinlets in ankerite veins.	
BGBST2012_212	MM179D	5502965	502300	699.33	699.54	Interlayered mudstone-sandstone	Interlayered mudstone-sandstone with calcitic alteration.	
BGBST2012_213	MM179D	5502965	502300	704.4	704.58	Iron formation with greenshale.	Interlayered green mudstone-iron formation with calcite alteration, pyrrhotite replaces iron formation. Veins have strong chlorite alteration selvage.	

Sample #	Drill Hole #	Coordinates Northing	Easting	Interval (m) from	to	Lithology	Reason	Reason II.
BGBST2012_214	MM179D	5502965	502300	705.48	705.71	Sandstone	Pyrite and trace arsenopyrite appear as dissemination around veins in sandstone or as vein filling in mudstone. Arsenopyrite rarely appears as coarse grained dissemination around veins in chlorite selvage.	
BGBST2012_215	MM179D	5502965	502300	718.73	719.02	mudstone	Abundant pyrrhotite appears as narrow veinlets in green mudstone.	
BGBST2012_216	MM179D	5502965	502300	714.42	714.76	Interlayered mudstone-sandstone	Quartz-calcite veins cut by calcite vein.	To define the order of the veins.
BGBST2012_217	MM179D	5502965	502300	720.48	720.72	Interlayered mudstone-sandstone	Weak sericite alteration haloe around quartz-calcite veins.	
BGBST2012_218	MM179D	5502965	502300	722.18	722.5	Sandstone	Average sandstone with calcite alteration.	
BGBST2012_219	MM179D	5502965	502300	723.16	723.43	Interlayered mudstone-sandstone	Quartz-calcite and quartz-calcite-chlorite-biotite veins with strong chlorite selvage.	
BGBST2012_220	MM179D	5502965	502300	724.34	724.72	Interlayered mudstone-sandstone	Calcite-chlorite vein overprinting an older quartz-calcite-ankerite? (pinkish) vein. These veins are associated with strong chlorite selvage.	
BGBST2012_221	MM179D	5502965	502300	731.83	732	Interlayered mudstone-sandstone	Calcite-sericite-chlorite alteration haloe around quartz-calcite veins. The alteration haloe contains fine-coarse grained pyrite, platy arsenopyrite and trace pyrrhotite and black biotite? Grains that seem to be overgrown by pyrrhotite and arsenopyrite.	
BGBST2012_222	MM179D	5502965	502300	736.33	736.54	Sandstone	Quartz-calcite-chlorite-pyrrhotite veins pyrrhotite-bearing chlorite-biotite selvage. Disseminated pyrite also appears in sandstone around the veins and trace in veins. No sericite alteration.	
BGBST2012_223	MM179D	5502965	502300	750.38	750.66	Interlayered mudstone-sandstone	Sericite-chlorite alteration haloe with pyrite. No pyrrhotite.	
BGBST2012_224	MM179D	5502965	502300	778.67	778.88	Dike? Sediment?	Strongly altered dike and maybe replaced porphyry grains but they seem to be emplaced parallel to bedding.	
BGBST2012_225	MM179D	5502965	502300	763.12	763.65	Interlayered mudstone-sandstone	Pyrrhotite mostly in chlorite/biotie? alteration haloe and minor in quartz-calcite vein. Pyrite also appears in this alteration haloe. Green mudstone hosts a vein of quartz-calcite-pyrrhotite with chlorite selvage. Green mudstone also contains disseminated pyrite, farther arsenopyrite and pyrrhotite. The sample also contains average sandstone.	
BGBST2012_226	MM179D	5502965	502300	783.7	784.35	Interlayered mudstone-sandstone-IF	K zone: Green mudstone with trace iron formation. The rock is affected by veins of quartz-ankerite, ankerite bands and by strong sericite alteration. 2-3 % disseminated pyrite in veins and in alteration haloe. Rare calcite veins. Moderate pyrite replacement in iron formation. Trace arsenopyrite and pyrrhotite.	K zone
BGBST2012_227	MM179D	5502965	502300	789.38	789.52	Sediment?	K zone	for vein study
BGBST2012_228	MM179D	5502965	502300	789.82	790	Sediment?	Coarse grained pyrite in ankerite-sericite? Alteration	K zone
BGBST2012_229	MM179D	5502965	502300	790.17	790.51	Sediment?	Coarse pyrite and carbonate emplaced in fine grained sediment?	K zone
BGBST2012_230	MM179D	5502965	502300	792.76	793.18	Iron formation with greenshale.	Strong sericite-calcite alteration haloe	
BGBST2012_231	MM179D	5502965	502300	797.71	797.95	Iron formation with greenshale.	Average interlayered jasper- and magnetite-rich iron formation.	

Sample #	Drill Hole #	Coordinates Northing	Easting	Interval (m) from	to	Lithology	Reason	Reason II.
BGBST2012_232	MM179D	5502965	502300	797	797.35	Iron formation with greenshale.	Pinkish quartz-ankerite/feldspar? Vein and light grey bleeching alteration haloe with probably magnetite grains.	
BGBST2012_233	MM179D	5502965	502300	802.07	802.22	Iron formation with greenshale.	Pyrite replacement in iron formation and disseminated arsenopyrite in greenshale.	
BGBST2012_234	MM179D	5502965	502300	803	803.35	Iron formation with greenshale.	Average green-grey mudstone with iron formation replaced by pyrite. Ankerite bands appear.	
BGBST2012_235	MM179D	5502965	502300	800.59	800.83	Iron formation with greenshale.	Average grey mudstone interlayered with reddish black iron formation. Small black, probably magnetite grains appear in mudstone.	
BGBST2012_236	MM179D	5502965	502300	813	813.24	Sandstone	Average sandstone with carbonate alteration and quartz-ankerite vein.	
BGBST2012_237	MM179D	5502965	502300	828.5	828.75	Iron formation with greenshale.	Iron formation interlayered with strongly calcitized green mudstone.	
BGBST2012_238	MM179D	5502965	502300	838	838.11	Iron formation with greenshale.	Interlayered iron formation-mudstone. Iron formation contains pyrite and calcite.	
BGBST2012_239	MM179D	5502965	502300	821.19	821.45	Mafic dike	Light green dike consists of 50 % white minerals and 50 % chlorite. It contains 2 % veins of quartz-ankerite/feldspar? And quartz-calcite, and all of them have chlorite selvage means the appearance of the white minerals is less abundant.	
BGBST2012_240	MM179D	5502965	502300	842.09	842.22	Interlayered mudstone-sandstone	Nonmineralized interlayered green mudstone-sandstone.	
BGBST2012_241	MM179D	5502965	502300	843.64	843.79	Interlayered mudstone-sandstone	Interlayered green mudstone-sandstone with one grain arsenopyrite in quartz-calcite vein.	
BGBST2012_242	MM106D	5503397	503577	429.4	429.62	Mafic dike	Yellowish grey mafic dike contains of 15-20 % white minerals (fsp?), 30 % black and light green chlorite in light grey? Matrix.	
BGBST2012_243	MM106D	5503397	503577	447.95	448.16	Mafic dike	Light grey mafic dike. It contains large, zonal, absolutely chloritized phenocrysts. Pseudomorph after pyroxene?	
BGBST2012_244	MM106D	5503397	503577	448.94	449.15	Mafic dike	Light grey mafic dike. It contains large, zonal, absolutely chloritized phenocrysts.	
BGBST2012_245	MM106D	5503397	503577	433.4	443.58	Sandstone	Quartz-ankerite-biotite-pyrite-pyrrhotite vein is cut by ankerite-biotite?-pyrite veinlet in fine grained sandstone.	
BGBST2012_246	MM106D	5503397	503577	461	461.2	Mafic dike	Dike containing of 30 % white minerals and 15-20 % chloritized phenocrysts in fine grained matrix	
BGBST2012_247	MM106D	5503397	503577	466.3	466.51	Interlayered mudstone-sandstone	Ankerite bands associated with disseminated pyrite are cut by quartz-ankerite?-chlorite veins. Black and green chlorite. Interlayered mudstone-sandstone.	
BGBST2012_248	MM106D	5503397	503577	491.48	491.65	Sandstone	Chlorite-rich sandstone with ankerite bands and veinlets. Average sandstone.	
BGBST2012_249	MM106D	5503397	503577	493.18	493.33	Dike? Sediment?	Strongly altered dike contact with ankeritic sediment.	
BGBST2012_250	MM106D	5503397	503577	500.64	500.74	Interlayered mudstone-sandstone	Quartz-ankerite vein cuts quartz-ankerite veins that has displacement along it. Weak ankerite haloe.	
BGBST2012_251	MM106D	5503397	503577	511.3	511.47	Interlayered mudstone-sandstone	Average, moderately ankeritized interlayered mudstone-sandstone. It shows a folded foliation and a new foliation formed parallel to the axial plane.	
BGBST2012_252	MM106D	5503397	503577	513.6	513.8	Mafic dike	Dike.	

Sample #	Drill Hole #	Coordinates Northing	Easting	Interval (m) from	to	Lithology	Reason	Reason II.
BGBST2012_253	MM106D	5503397	503577	553.6	553.78	Sediment?	Strong green-yellow alteration haloe of presumably chlorite and minor fuchsite appears at the contact of a dike emplaced in sediment.	
BGBST2012_254	MM106D	5503397	503577	552.23	552.46	Interlayered mudstone-sandstone	Disseminated pyrite associated with strong ankerite alteration haloe around a quartz-ankerite vein in sediment.	
BGBST2012_255	MM106D	5503397	503577	566.06	566.53	Interlayered mudstone-sandstone	Quartz-ankerite vein cuts across quartz-ankerite veins and a young ankerite-pyrite vein cut through everything else and have bleeching haloe around them.	
BGBST2012_256	MM106D	5503397	503577	579.2	579.59	Interlayered mudstone-sandstone	Average mudstone and sandstone with moderate ankerite alteration and bands.	
BGBST2012_257	MM106D	5503397	503577	583.96	584.17	Mafic dike	Dike consists of 30-40 % yellow and pink phenocrysts, 30-40 % chlorite and 20-30 % fine grained phenocrysts.	
BGBST2012_258	MM106D	5503397	503577	596.63	597	Interlayered mudstone-sandstone-IF	Iron formation quartz-ankerite-chlorite-pyrite vein with moderate ankerite alteration haloe.	
BGBST2012_259	MM106D	5503397	503577	610.4	610.53	Iron formation	Average iron formation with presumably ankerite-pyrite veinlets emplaced parallel to the bedding.	
BGBST2012_260	MM106D	5503397	503577	617.01	617.26	Iron formation	Iron formation with sedimentary dike.	
BGBST2012_261	MM106D	5503397	503577	620.41	620.68	Mafic dike	Dark green mafic dike with pinkish green vein.	
BGBST2012_262	MM106D	5503397	503577	628.41	628.69	Mafic dike	Green-brownish grey mafic dike. Same as earlier. It contains pinkish (ankerite?) patches and veins that can be cut by quartz-ankerite? Veins associated with chlorite selvage.	
BGBST2012_263	MM106D	5503397	503577	633.36	633.54	Mafic dike	Same dike with other quartz-ankerite veins associated with bleaching and chlorite alteration haloe.	
BGBST2012_264	MM106D	5503397	503577	655.48	655.63	Mafic dike	Average biotite?/two types of chlorite?-bearing mafic dike.	
BGBST2012_265	MM106D	5503397	503577	655.71	656.2	Mafic dike	Quartz-ankerite veins associated with strong chlorite-sericite?-fuchsite alteration haloe.	
BGBST2012_266	MM106D	5503397	503577	646.11	646.33	Mafic dike	Quartz-ankerite-chlorite-pyrite veins in biotite?-bearing rock.	
BGBST2012_267	MM106D	5503397	503577	627.6	627.75	Mafic dike	Average mafic dike without biotite/brownish chlorite.	
BGBST2012_268	MM106D	5503397	503577	657.52	657.9	Porphyry	Strong green (sericite) pyrite-bearing alteration haloe around quartz-ankerite? Veins in porphyry	
BGBST2012_269	MM106D	5503397	503577	658.8	659.27	Porphyry	Strong sericite alteration haloe around quartz-ankerite? Veins with gradual change.	
BGBST2012_270	MM106D	5503397	503577	664.31	664.74	Mafic dike	Greenish alteration haloe around quartz-ankerite veins in mafic dike.	
BGBST2012_271	MM106D	5503397	503577	666.4	666.85	Porphyry	Two generations of quartz-ankerite veins with strong alteration haloe in porphyry.	
BGBST2012_272	MM106D	5503397	503577	669.6	670.21	Mafic dike	Strong alteration haloe in mafic dike.	
BGBST2012_273	MM106D	5503397	503577	675	675.42	Porphyry	Strong green alteration haloe in porphyry with pyrite around quartz-ankerite veins. According to Premier's log, a speck of gold was observed in this interval.	
BGBST2012_274	MM106D	5503397	503577	678.19	678.36	Mafic dike	Average, nonmineralized mafic dike.	
BGBST2012_275	MM106D	5503397	503577	678.53	678.77	Porphyry	Average, nonmineralized porphyry.	
BGBST2012_276	MM106D	5503397	503577	702.62	702.83	Interlayered mudstone-sandstone-IF	Average iron formation with different? Types of pyrite and a late quartz-ankerite? Vein.	
BGBST2012_277	MM106D	5503397	503577	704.1	704.24	Interlayered mudstone-sandstone-IF	Late, pyrite-bearing vein in an average mudstone-sandstone.	
BGBST2012_278	MM106D	5503397	503577	704.3	704.44	Interlayered mudstone-sandstone-IF	Average sediment with ankerite alteration and vein.	

Sample #	Drill Hole #	Coordinates Northing	Easting	Interval (m) from	to	Lithology	Reason	Reason II.
BGBST2012_279	MM106D	5503397	503577	709.6	710.02	Mafic dike	Abundant quartz-ankerite veining at the upper contact of the mafic dike.	
BGBST2012_280	MM106D	5503397	503577	713.75	713.92	Mafic dike	Strong yellow alteration in mafic dike at the contact with iron formation.	
BGBST2012_281	MM106D	5503397	503577	714.7	714.86	Interlayered mudstone-sandstone-IF	Bleaching and ankerite alteration in mudstone-sandstone with trace iron formation. Average below the dike.	
BGBST2012_282	MM106D	5503397	503577	717.19	717.43	Interlayered mudstone-sandstone-IF	Semi-massive pyrite appears as replacement of iron formation and subordinately veinfilling.	
BGBST2012_283	MM106D	5503397	503577	730.45	730.65	Interlayered mudstone-sandstone	Nonmineralized strongly altered mudstone-sandstone.	
BGBST2012_284	MM106D	5503397	503577	731.82	732.24	Interlayered mudstone-sandstone	Vein gold-bearing quartz-ankerite vein with alteration haloe that contains disseminated pyrite and trace arsenopyrite.	
BGBST2012_285	MM106D	5503397	503577	733.67	734.24	Interlayered mudstone-sandstone-IF	Quartz-ankerite veins associated with chlorite-ankerite alteration in iron formation and mudstone-sandstone. It contains minor iron formation replaced by pyrite and arsenopyrite. No penetrating sericite alteration.	
BGBST2012_286	MM106D	5503397	503577	737.64	737.88	Interlayered mudstone-sandstone	Folded quartz-ankerite vein associated with bleaching and sericite alteration haloe that contains disseminated sulphide.	
BGBST2012_287	MM106D	5503397	503577	739.08	739.48	Interlayered mudstone-sandstone	Moderate-strong alteration in mudstone-sandstone. Preserved, older alteration and alteration haloe.	
BGBST2012_288	MM106D	5503397	503577	722.67	722.83	Interlayered mudstone-sandstone-IF	Iron formation replaced by pyrite along a quartz-ankerite vein.	
BGBST2012_289	MM106D	5503397	503577	748.1	748.39	Interlayered mudstone-sandstone-IF?	Broken, preasumably altered iron formation with carbonate?-sulphide (arsenopyrite+?) as cementation.	
BGBST2012_290	MM106D	5503397	503577	749.1	749.9	Interlayered mudstone-sandstone-IF?	Breccia.	
BGBST2012_291	MM106D	5503397	503577	750.42	750.68	Diabase?	Black, fine grained dike.	
BGBST2012_293	MM106D	5503397	503577	766.91	767.41	Interlayered mudstone-sandstone	Quartz-ankerite vein with pyrite- and minor pyrrhotite-bearing bleaching alteration haloe.	
BGBST2012_294	MM106D	5503397	503577	768.48	769	Interlayered mudstone-sandstone	Pyrite is getting semi-massive in association with quartz-ankerite veins, but no gold. Pyrite also appears in the neck of boudins of quartz-ankerite veins.	
BGBST2012_295	MM106D	5503397	503577	773.75	773.87	Iron formation with greenshale.	Average iron formation with bleaching. Arsenopyrite in green mudstone and iron formation. Ankerite alteration.	
BGBST2012_296	MM106D	5503397	503577	774.53	774.7	Interlayered mudstone-sandstone-IF	Fractures filled with semi-massive pyrite associated with quartz-ankerite vein.	
BGBST2012_297	MM106D	5503397	503577	778.76	779.2	Iron formation with greenshale.	Average sediment with quartz-ankerite veins and a speck of gold.	
BGBST2012_298	MM106D	5503397	503577	770.9	771.2	Iron formation with greenshale.	Quartz-ankerite?-chlorite vein with semi-massive pyrite in vein and alteration haloe. Disseminated pyrrhotite appears in the sediment farther from veins.	
BGBST2012_299	MM106D	5503397	503577	781.02	781.87	Semi-massive sulphide	Massive sulphide replacement (py>po) associated quartz-ankerite veins and very strong bleaching.	
BGBST2012_300	MM106D	5503397	503577	785.33	786	Semi-massive sulphide	Semi-massive pyrite and arsenopyrite without gold.	
BGBST2012_301	MM106D	5503397	503577	788	788.3	Iron formation with greenshale.	Chlorite-sericite alteration haloe around quartz-ankerite veins with pyrite, arsenopyrite and trace pyrrhotite.	
BGBST2012_302	MM106D	5503397	503577	784.96	785.16	Iron formation	Average nonmineralized iron formation.	

Sample #	Drill Hole #	Coordinates Northing	Easting	Interval (m) from	to	Lithology	Reason	Reason II.
BGBST2012_303	MM106D	5503397	503577	789.05	789.41	Interlayered mudstone-sandstone	Average mudstone-sandstone between mineralized zones.	
BGBST2012_304	MM106D	5503397	503577	797.2	797.76	Semi-massive sulphide	Semi-massive pyrite-pyrrhotite-arsenopyrite associated with quartz-ankerite veins and very strong bleaching haloe.	
BGBST2012_305	MM106D	5503397	503577	800.8	801	Semi-massive sulphide	Semi-massive pyrite≈pyrrhotite> arsenopyrite.	
BGBST2012_306	MM106D	5503397	503577	805.6	805.81	Semi-massive sulphide	Semi-massive pyrite-arsenopyrite.	
BGBST2012_307	MM106D	5503397	503577	807	807.3	Semi-massive sulphide	Pyrite-pyrrhotite > arsenopyrite associated with with quartz-ankerite veins in iron formation. Pyrrhotite is overgrown by pyrite and arsenopyrite. Is apy overgrown by pyrite?	
BGBST2012_308	MM106D	5503397	503577	813.2	813.32	Semi-massive sulphide	Pyrite and arsenopyrite overgrows pyrrhotite in alteration haloe of a quartz-ankerite-chlorite vein	
BGBST2012_309	MM106D	5503397	503577	815.31	815.49	Semi-massive sulphide	Folded semi-massive pyrite>arsenopyrite>pyrrhotite. Pyrite seems to overgrow arsenopyrite associated with quartz-ankerite-chlorite vein that have chlorite-sericite alteration haloe.	
BGBST2012_310	MM106D	5503397	503577	818.95	819.58	Semi-massive sulphide	This represents the entire semi-massive mineralization consists of fine-coarse grained pyrite and arsenopyrite.	
BGBST2012_311	MM106D	5503397	503577	822	822.18	Semi-massive sulphide	Semi-massive pyrite, pyrrhotite and arsenopyrite.	
BGBST2012_312	MM106D	5503397	503577	826.24	826.5	Iron formation and semi-massive sulphide	Brecciated iron formation and quartz-ankerite veins.	Relationship between sulphides and brecciation.
BGBST2012_313	MM106D	5503397	503577	827.2	827.38	Iron formation with greenshale.	Average jasper- and magnetite-rich iron formation interlayered with bleached sediment. Pyrite stringers.	
BGBST2012_314	MM106D	5503397	503577	834.98	835.34	Iron formation with greenshale.	Average interlayered mudstone-fine grained sandstone with quartz-ankerite veins have disseminated sulphide-bearing bleaching and sericite alteration haloe.	
BGBST2012_315	MM106D	5503397	503577	840.31	840.51	Semi-massive sulphide	Last semi-massive pyrite associated with quartz-ankerite veins with moderate alteration haloe.	
BGBST2012_316	MM106D	5503397	503577	840.8	841.5	Iron formation with greenshale.	Quartz-ankerite veins can have bleaching and sericite haloe around them that also contains disseminated pyrite and pyrite stringers.	
BGBST2012_317	MM106D	5503397	503577	848.17	848.4	Iron formation with greenshale.	Quartz-ankerite veins with pyrite(stringers)-bearing chlorite selvage.	
BGBST2012_318	MM106D	5503397	503577	897.38	897.55	Interlayered mudstone-sandstone-IF	Quartz-ankerite vein with moderate bleaching and chlorite alteration haloe. Pyrite and pyrrhotite appear in vein in mudstone.	
BGBST2012_319	MM106D	5503397	503577	899.73	900	Interlayered mudstone-sandstone	Average ankerite alteration in mudstone-sandstone.	
BGBST2012_320	MM106D	5503397	503577	902.28	902.75	Sandstone	Quartz-ankerite vein with ankerite alteration haloe in sandstone with disseminated pyrite and pyrrhotite.	
BGBST2012_321	MM106D	5503397	503577	940.05	940.38	Interlayered mudstone-sandstone	Average green mudstone-sandstone.	
BGBST2012_322	MM106D	5503397	503577	946.3	946.51	Iron formation	Average iron formation.	
BGBST2012_323	MM106D	5503397	503577	969	969.19	Iron formation	Possibly refolded fold in iron formation	
BGBST2012_324	MM106D	5503397	503577	973	973.27	Iron formation	Refolded? Jasper-rich iron formation	
BGBST2012_325	MM106D	5503397	503577	973.71	973.86	Iron formation	Refolded!! Jasper-rich iron formation	
BGBST2012_326	MM106D	5503397	503577	974.6	974.75	Iron formation	Average, tightly folded jasper-rich iron formation	

Sample #	Drill Hole #	Coordinates Northing	Easting	Interval (m) from	to	Lithology	Reason	Reason II.
BGBST2012_327	MM106D	5503397	503577	975.2	975.33	Iron formation	Transposed quartz-biotite-hematite vein in jasper-rich iron formation.	
BGBST2012_328	MM106D	5503397	503577	984.73	984.93	Interlayered mudstone-sandstone-IF	Quartz-carbonate+hematite? Vein with bleaching-chlorite-sericite alteration haloe	
BGBST2012_329	MM106D	5503397	503577	985.78	985.9	Iron formation	Quartz-hematite-carbonate vein and small sedimentary dike in iron formation.	
BGBST2012_330	MM106D	5503397	503577	990	990.46	Interlayered mudstone-sandstone-IF	Bleached sandstone	Semi-massive pyrite and pyrite stringers in iron formation and green mudstone
BGBST2012_331	MM106D	5503397	503577	992.9	993.16	Iron formation with greenshale and semi massive pyrite	Semi-massive pyrite in green mudstone and iron formation	
BGBST2012_332	MM106D	5503397	503577	993.61	994.21	Interlayered mudstone-sandstone-IF	Semi-massive pyrite and arsenopyrite, overgrowing texture! Py texture with transposed, boudinaged vein.	
BGBST2012_333	MM106D	5503397	503577	995.09	995.35	Iron formation with greenshale.	Average interlayered iron formation-green mudstone with disseminated pyrite.	
BGBST2012_334	MM106D	5503397	503577	996.61	996.81	Interlayered mudstone-sandstone-IF	Semi-massive fine-coarse grained arsenopyrite-pyrite associated with quartz vein.	Overgrowing relationship between pyrite and arsenopyrite.
BGBST2012_335	MM106D	5503397	503577	1002.86	1003.15	Sandstone	Average calcitized sandstone with quartz-calcite-biotite-pyrite-pyrrhotite with weak chlorite selvage.	
BGBST2012_336	MM106D	5503397	503577	1012.35	1012.5	Interlayered mudstone-sandstone	Quartz-carbonate-biotite vein associated with weak chlorite selvage with disseminated pyrite and pyrrhotite.	
BGBST2012_337	MM106D	5503397	503577	1026.6	1026.84	Interlayered mudstone-sandstone	Quartz-calcite vein with pyrrhotite that is overgrown by pyrite in green mudstone-sandstone.	
BGBST2012_338	MM106D	5503397	503577	1036.41	1036.56	mudstone	Average calcitized mudstone.	
BGBST2012_339	MM106D	5503397	503577	1052.53	1052.77	Sandstone	Average ankerite alteration in sandstone.	
BGBST2012_340	MM106D	5503397	503577	1060.34	1060.43	Sandstone	Quartz-ankerite-calcite-biotite-pyrite-pyrrhotite in ankeritic sandstone.	
BGBST2012_341	MM106D	5503397	503577	1070.19	1070.42	mudstone	Average ankeritized mudstone.	